

# Low-Coordinate Hypervalent Phosphorus<sup>†,‡</sup>

Anthony J. Arduengo, III<sup>§,\*</sup> and Constantine A. Stewart<sup>||,\*</sup>

DuPont Science and Engineering Laboratory, Experimental Station, Wilmington, Delaware 19880-0328, and Himont, U.S.A., Inc., Research and Development Center, Elkton, Maryland 21921

Received November 8, 1993 (Revised Manuscript Received February 8, 1994)

## Contents

I. Introduction	1215
II. Ligand Design	1216
III. Synthesis	1217
IV. Valence-Bond Descriptions of ADPnO	1217
V. Calculated Geometries and Energies	1219
VI. Edge Inversion	1221
VII. Oxidative Additions of HX Compounds to ADPO	1223
A. Protonations of ADPO and Related Molecules	1223
B. Hydrolysis of ADPO	1226
C. Oxidative Additions of Halogens	1226
D. Reactions of ADPO with Dicarbonyl Compounds	1227
E. Reactions of ADPO with Hexafluoro-2-butyne	1228
F. Six-Coordinate Phosphorus System	1229
VIII. Nuclear Magnetic Resonance Spectra	1229
IX. Transition Metal Complexes	1230
A. Complexes with the Transition Group 6 Metals, Cr and W	1230
B. Complexes with the Transition Group 7 Metal, Mn	1230
C. Complexes with the Transition Group 8 Metals, Fe and Ru	1231
D. Complexes with the Transition Group 10 Metals, Ni, Pd, and Pt	1232
E. Complexes with the Transition Group 11 Metal, Ag	1234
X. Conclusions	1235
XI. Abbreviations	1236
XII. References	1236

## I. Introduction

This review marks 10 years of research into the chemistry of low-coordinate hypervalent phosphorus compounds.<sup>1</sup> The first tricoordinated hypervalent phosphorus compound, 10-P-3<sup>2</sup>3,7-di(*tert*-butyl)-5-aza-2,8-dioxo-1-phosphabicyclo[3.3.0]octa-2,4,6-triene (AD-PO),<sup>3</sup> was reported in 1983.<sup>4</sup> Another type of 10-P-3 intermediate, **1**, was discovered by Schmidpeter and Lochschmidt in this same time frame.<sup>5</sup>

The work by Schmidpeter *et al.* and Arduengo *et al.* represent two different ligand designs to stabilize the

<sup>†</sup> In memory of Linus Amadeus and Schroeder.

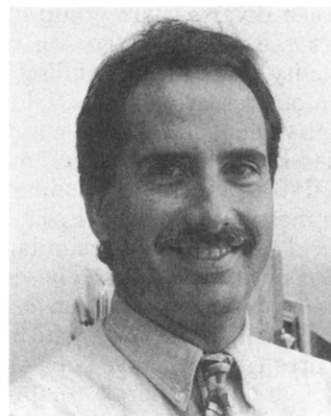
<sup>‡</sup> Contribution no. 6745 from DuPont Science and Engineering Laboratory.

<sup>§</sup> DuPont.

<sup>||</sup> Himont.

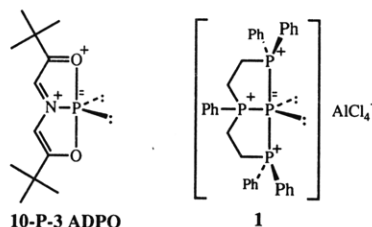


Anthony J. Arduengo, III (b 1952) was raised in Atlanta, GA. He received the Bachelor of Science degree (with honor) in chemistry from The Georgia Institute of Technology (1974) and Ph.D. in organic chemistry from the same institution in 1976. After a year in industry with DuPont's Central Research Department, he joined the organic chemistry faculty of The University of Illinois—Urbana. In 1984 he returned to DuPont where he has held various positions and is currently a Research Leader in the Polymer Science Section of the Central Science and Engineering Laboratory. He has served on the editorial boards of *Chemical Reviews* and *Heteroatom Chemistry* as well as the IUPAC commission on inorganic nomenclature. His research interests are broadly in the area of main group element chemistry with particular interest in compounds with unusual valence. Hobbies include trumpet playing, bicycling, antique cars, and classical music.



Constantine A. Stewart was born in 1957 in San Angelo, TX. He received his Bachelor of Arts in chemistry (1980) from Texas Tech University in Lubbock, TX, and his Ph.D. in inorganic chemistry from the University of Texas at Austin (1984). He spent two years as a Visiting Research Scientist at Central Research and Development at DuPont. In 1986 he joined Himont U.S.A., Research and Development. He is currently working in the field of Ziegler-Natta catalysis. His hobbies include bicycling and photography.

T-shaped 10-P-3 geometry. Both designs employ a bicyclic five-membered ring effect to stabilize an axial-equatorial-axial chelation of the central pseudo-trigonal



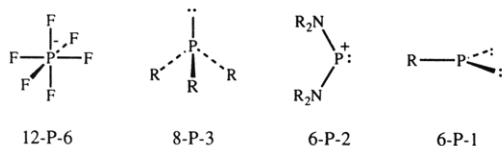
bipyramidal ( $\psi$ -tbp) phosphorus. Each of these ligands has a different atom in the axial positions ( $P^+$  or  $O$ ). The atom in the apical position of a  $\psi$ -tbp structure must be effectively electronegative in order to accommodate the increased electron density in these positions and thus stabilize the linear three-center, four-electron (hypervalent) bond. It seems likely that oxygen and phosphonium centers would differ in this regard. The two ligands also differ in charge type. The ligand system of 10-P-3 ADPO compensates for the *formally*<sup>6</sup> dianionic charge at phosphorus. The ligand system employed in **1** does not match the formal charge at the 10-P-3 center and thus produces a cationic fragment. These differences may account for why the 10-P-3 structure in **1** is a transition state while 10-P-3 ADPO is a minimum on the potential energy surface. We will focus the rest of our discussion on molecules with a 10-P-3 ground-state structure.

The chemistry of 10-P-3 ADPO has grown considerably over the last 10 years. Many new structures and bonding arrangements have been synthesized and characterized and a new mechanism for inversion of the main group compounds has been explored. Novel transition metal complexes have been prepared and characterized. It is the aim of this review to summarize the knowledge that has resulted from the study of 10-P-3 ADPO and related molecules.

In 1980 Martin and Arduengo developed the "N-X-L" system to categorize compounds according to their valence electron count and coordination number.<sup>2</sup> This N-X-L system has been very useful in studying relationships between diverse main group element compounds. In fact, the N-X-L system was used by us to predict the stability of the 10-P-3 bonding arrangement and thus began our research in this field.

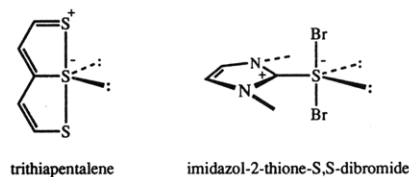
Typically, high valence electron counts at phosphorus are accompanied by high coordination numbers. For example the 12-P-6 arrangement is commonly found in the hexafluorophosphate anion ( $PF_6^-$ ). Low valence electron counts at phosphorus are similarly accompanied by low coordination numbers. The very abundant phosphines are representatives of an 8-P-3 bonding arrangement. Phosphenium ions, which represent a 6-P-2 bonding arrangement, have been observed<sup>7</sup> and even one-coordinate phosphorus compounds, phosphinidenes (6-P-1), have been postulated as intermediates (Scheme 1).<sup>8</sup>

#### Scheme 1



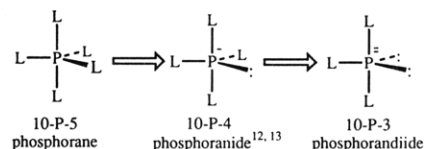
It was the aim of our research with the ADPO systems to combine a relatively high electron count with a

relatively low coordination number. In this regard, the first opportunity for a new structure arises with the 10-P-3 bonding arrangement. This unusual arrangement for phosphorus has been observed for sulfur where a variety of 10-S-3 compounds are known (*e.g.* the trithiapentalenes<sup>9,10</sup> and thione *S,S*-dihalides<sup>11</sup>).



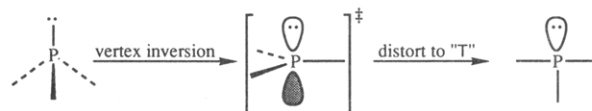
These sulfur structures suggest that the 10-P-3 compounds should exhibit a T-shaped pseudo-trigonal bipyramidal geometry ( $\psi$ -tbp). Formally, the  $\psi$ -tbp 10-P-3 geometry also is obtained by successive replacement of equatorial ligands of a 10-P-5 phosphorane with lone pairs of electrons (Scheme 2).

#### Scheme 2



The planar T-shaped geometry of a 10-P-3 center can also be viewed as a distortion of the trigonal planar 8-P-3 structure of the transition state for phosphine inversion (Scheme 3). This relates the normal vertex

#### Scheme 3

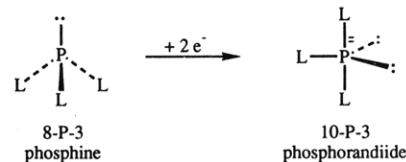


inversion of pyramidal 8-P-3 phosphines to the planar T-shaped structure of the ADPO compounds.<sup>14,15</sup> This relationship will be discussed later in more detail.

## II. Ligand Design

Conceptually a 10-P-3 species can be viewed as a two-electron reduction of the common 8-P-3 center (Scheme 4). This reduction affords the *formally* dianionic

#### Scheme 4

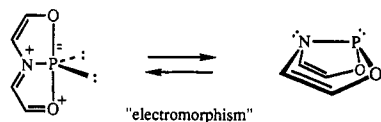


phosphorus center of the 10-P-3 arrangement. To stabilize this unusual structure a special ligand design is needed.

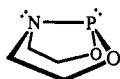
A tridentate diketo amine ligand was chosen as a means to stabilize the 10-P-3 bonding system. This ligand provides the following characteristics: (1) powerful reducing ability, (2) internal charge compensation for the *formally* dianionic phosphorus center, (3) five-membered ring linkage of apical and equatorial sites of the  $\psi$ -tbp geometry,<sup>16,17</sup> and (4) electronegative atoms

in the apical positions. The general synthesis, using the diketoamine and phosphorus trichloride to give the 3,7-dialkyl-5-aza-2,8-dioxo-1-phosphabicyclo[3.3.0]octa-2,4,6-triene (ADPO) is discussed below (*vide infra* eq 1). The analogous arsenic<sup>18</sup> and antimony<sup>19</sup> compounds have been synthesized by similar procedures.

The ligand designed for the ADPO ring system allows an interesting opportunity to observe two different potential ground-state structures, the intended planar 10-P-3 arrangement or the alternative more classical, folded 8-P-3 arrangement.



The special relationship between these isomers that are related by having the same overall connectivity but different geometries as a result of electron redistribution has been referred to as "electromorphism".<sup>20</sup> The folded 8-P-3 electromorph can be found in many related structures in the work of Wolf and co-workers.<sup>21-24</sup>

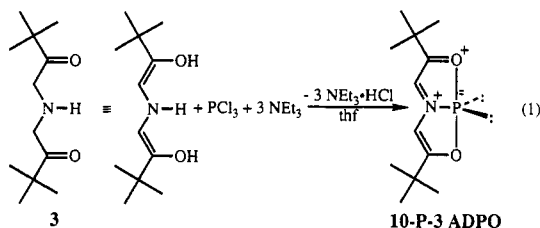


2

There is substantial spectroscopic evidence that supports a folded geometry for the saturated bicyclic compounds **2** of Wolf.<sup>21,24</sup> The lack of a  $\pi$ -system in these compounds makes it unlikely that any sort of planar T-shaped arrangement could be an important ground-state structure. The consideration of the saturated structures with folded geometries (like **2**) makes the planar 10-P-3 ADPO arrangement seem quite remarkable. However, there are a number of electronic and structural features in the ADPO ring system that favor a planar 10-P-3 arrangement.

### III. Synthesis

The ADPO ring system is easily synthesized by condensation of a diketoamine ligand, **3**, with a phosphorus trihalide in the presence of 3 equiv of a base (eq 1).<sup>25</sup>

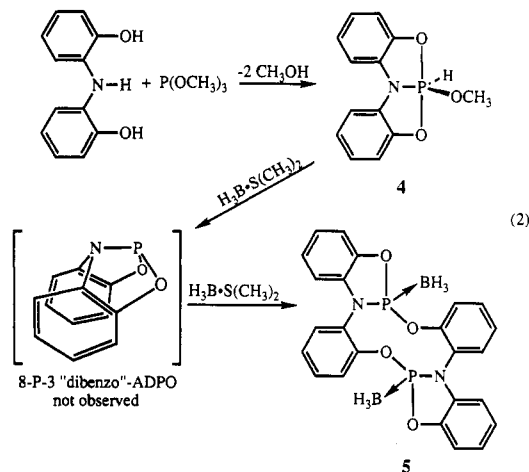


3

10-P-3 ADPO

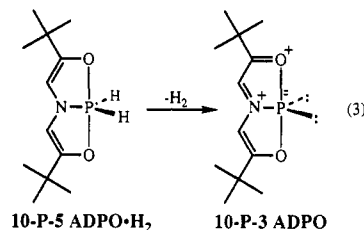
A variant of this approach has also been used with *O,O'*-dihydroxyphenylamines (eq 2). In this latter case the "dibenzo"-ADPO ring system was not isolated, but rather the methanol adduct **4** (eq 2).<sup>26</sup> Attempts to form a "dibenzo"-ADPO ring system by elimination of methanol from **4** with borane have led only to the isolation of the bis(borane) adduct of the cyclic dimer, **5** (eq 2).<sup>26,27</sup> This apparent lack of stability of planar 10-P-3 "dibenzo"-ADPO is consistent with the close

energetic relation between planar 10-P-3 ADPO and folded 8-P-3 ADPO (*vide infra*). The relative energetics of 10-P-3 and 8-P-3 "dibenzo"-ADPO could be inverted, and dimerization may be quite rapid relative to ADPO (as in the saturated analogs like **2**). It is not known whether the borane catalyzes the dimerization of "dibenzo"-ADPO or forms an adduct with the dimer after it is formed (some transition metals can catalyze ADPO dimerization, *vide infra*).

8-P-3 "dibenzo"-ADPO  
not observed

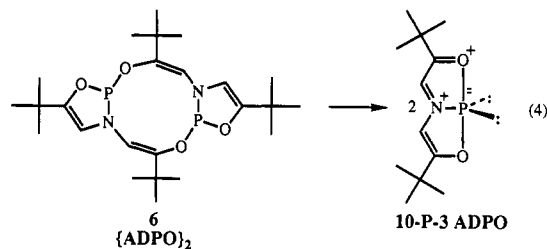
5

The 10-P-3 ADPO ring system is also formed by the reductive elimination of hydrogen from the phosphorane, ADPO·H<sub>2</sub>, *vide infra* (eq 3).

10-P-5 ADPO·H<sub>2</sub>

10-P-3 ADPO

The tricyclic ring system, **6**, which is a dimer of ADPO ({ADPO}<sub>2</sub>)<sup>28</sup>, undergoes a slow conversion to the bicyclic ADPO ring system (*vide infra*) (eq 4).

{ADPO}<sub>2</sub>

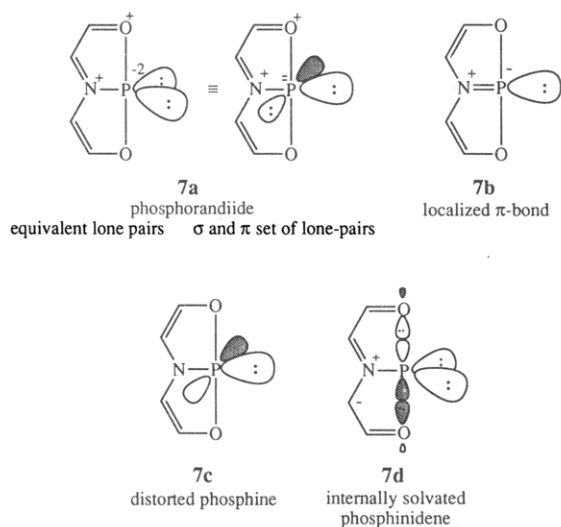
10-P-3 ADPO

These latter two routes are of little utility since the starting materials (ADPO·H<sub>2</sub> and {ADPO}<sub>2</sub>) are indirectly derived from 10-P-3 ADPO.

### IV. Valence-Bond Descriptions of ADPO

Several various extreme bonding descriptions have been presented to describe the low-coordinate hypervalent phosphorus in the ADPO ring system.<sup>14</sup> At this point it is beneficial to review these descriptions. A number of different valence bond structures with brief descriptions are shown in Scheme 5.

## Scheme 5



The structures of **7a** are equivalent and differ only in the description of the lone pairs of electrons. These lone pairs are either equivalent ( $sp^2$ -like hybrid orbitals) or reside in a  $\sigma$ - and  $\pi$ -set of orbitals ( $sp$ - and  $p$ -like). Structures **7b** and **7c** are different from **7a** in the localization of electron density. Structure **7c** suggests that the two-electron reduction of the phosphorus arising from transfer of electron density from the ligand backbone to the phosphorus did not occur. Structure **7b** indicates that the  $\pi$ -bonding in the ligand backbone is localized and there is an N–P double bond. Structure **7d** is actually an alternative representation of structure **7a** which is intended to emphasize the “internal solvation” character of a hypervalent bond. As such, structure **7d** will be discussed separately.

Consideration of structure **7c** as a viable contributor to the valence bond description of 10-P-3 ADPO can be ruled out for several reasons. Because structure **7c** is planar, participation of the out-of-plane phosphorus  $p$ -orbital in the  $\sigma$ -bonding system about the phosphorus center is prohibited due to symmetry considerations. The P–N bond and phosphorus in-plane lone pair electrons use the in-plane phosphorus  $p$ -orbital and  $s$ -orbital to accommodate these valence electrons. The O–P–O bonding manifold is a linear three-center, four-electron (3c,4e) hypervalent bond utilizing the remaining  $p$ -orbital at phosphorus. The vacant  $p$ -orbital on phosphorus and the electron-rich 3c,4e hypervalent bond are incompatible. This incompatibility could be expected to cause the structure to relax to a folded geometry that would allow mixing of the vacant  $p$ -orbital on phosphorus with the orbitally deficient hypervalent bond. This would transform structure **7c** to a seemingly more stable folded 8-P-3 arrangement as found in the saturated compounds of Wolf, **2**. In fact, this out-of-plane folding points to structure **7c** as the transition state for an edge inversion process (*vide infra*).<sup>15</sup> The identity of structure **7c** as a transition state requires that it cannot be used to represent a planar ground-state structure.

Since the bonding scheme of **7c** cannot be important in a ground-state structure it is reasonable to assume that there is some electron density in the out-of-plane  $p$ -orbital. By neglecting the importance of bonding scheme **7c**, this places more importance on structure

**7a**. But is the 10-P-3 ADPO structure best represented by **7a** or **7a** + **7b** or **7b** + **7c**? *Ab initio* calculations support the description of a delocalized out-of-plane phosphorus lone pair of electrons. The heavier analogs of the ADPO structure in which the phosphorus has been replaced by arsenic or antimony are known and serve as reference points for the question of  $\pi$ -delocalization and electron density in the out-of-plane  $p$ -orbital at the pnictogen center.

The  $\pi$ -overlap-based delocalization would be expected to be greatest for phosphorus and the least for antimony on the basis of atom sizes. The 10-Sb-3 ADSbO molecule is best described by **7a**. These trends in  $\pi$ -delocalization are also supported by calculation of the atomic charges in 10-P-3 ADPO and 10-As-3 ADAso. The out-of-plane electron density at the pnictogen center is necessary to obtain the planar 10-Pn-3 arrangement. Arsenic and antimony retain more of this  $p$ - $\pi$  density as a result of their diminished ability to enter into  $p$ - $\pi$  bonding with the neighboring nitrogen and oxygen centers. It is of interest to note that the stability of the planar phosphorus system actually suffers due to the increasing importance of P–N and P–O  $p$ - $\pi$  interactions.

The NMR spectra of the 10-Pn-3 ADPnO molecules also support these trends in the degree of delocalization. The charge separation increases from ADPO to ADSbO, supporting a more localized structure of the latter. On the basis of the <sup>15</sup>N shifts of the ADPnO series structures **7a** and **7b** are better representations than **7c** due to the large iminium character of the nitrogen ( $\delta \sim -100$  ppm).<sup>29</sup> In addition, the <sup>1</sup>H, <sup>13</sup>C, and <sup>17</sup>O shifts are more consistent with structure **7a** than either **7b** or **7c**.<sup>30</sup>

The calculations and NMR observations, in conjunction with the X-ray structures, indicate the importance of valence bond representation **7a**. The lengths of the P–N bonds in the 10-P-3 ADPO molecule (Table 1) are comparable to common equatorial single bonds in typical 10-P-5 centers.<sup>31</sup> Thus, the P–N bond distance does not suggest any multiple bonding character between phosphorus and nitrogen in the 10-P-3 ADPO molecule which would be required in structure **7b**.

Without invoking high-energy 3d-orbitals at phosphorus, the hypervalent bond in **7a** cannot be eliminated by reassigning the valence  $s$ - and  $p$ -orbital functions at phosphorus. Ten electrons must be accommodated between the two lone pairs of electrons (4e) and three  $\sigma$ -bonds (6e). The lone pairs of electrons require one atomic (or molecular) orbital each. Each two-center, two-electron (2c,2e)  $\sigma$ -bond will require two atomic orbitals (forming two molecular orbitals,  $\sigma$  and  $\sigma^*$ ). If three 2c,2e-bonds are formed, six orbital functions are needed. The total of two lone pairs and three 2c,2e-bonds requires eight orbital functions. Phosphorus can contribute four valence orbitals (1s and 3  $p$ 's), and each of the attached atoms can contribute one additional  $\sigma$ -orbital function for a total of seven basis functions. Thus, the phosphorus system is orbitally deficient if it must consist of three 2c,2e-bonds and two lone pairs. If, on the other hand, three centers participate in a 3c,4e hypervalent bond, only three (rather than four) orbital functions are needed to form two of the  $\sigma$ -bonds reducing the total number of orbitals required to seven.

This hypervalent O–P–O bond is exemplified in structure **7d**. This structure represents a singlet

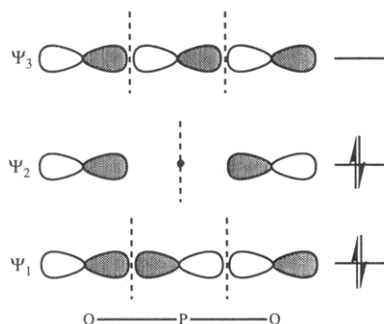
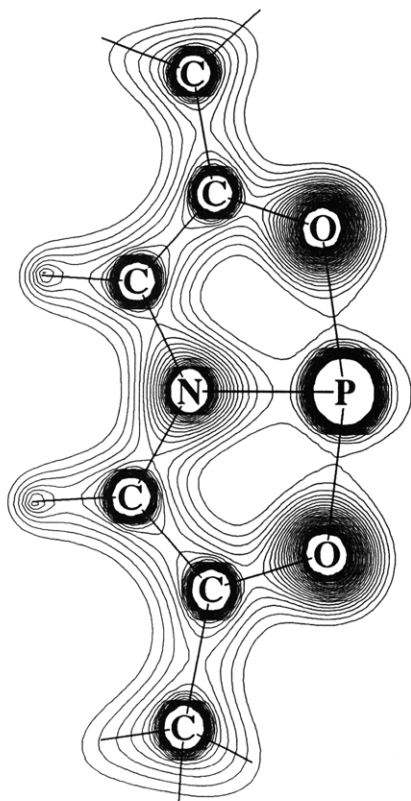


**Figure 1.** Simple valence orbital description of the 3c,4e hypervalent bond.

phosphinidene (6-P-1) which is internally solvated by the two carbonyl groups. The interaction of the oxygen lone pairs from the carbonyl oxygens with the empty p-orbital at phosphorus is the same type of interaction found in the lowest lying molecular orbital ( $\Psi_1$ ) of the linear 3c,4e bond (Figure 1).

The representation of the hypervalent bond at phosphorus as a phosphinidene solvated internally by the oxygens of an azomethine ylide (7d) is also suggested by the total electron density in the plane of the molecule. The total electron density in the molecular plane of 10-P-3 ADPO is illustrated by the following ADPO drawing:<sup>32</sup>



At the contour levels shown ( $0.75 \rightarrow 10 \text{ e}\text{\AA}^{-3}$ ) the density in the hypervalent bond has just vanished while the other  $\sigma$ -bonds are still readily apparent.

This internally solvated phosphinidene representation of the 10-P-3 ADPO structure also underscores the oxidation state the phosphorus in 10-P-3 ADPO which is I.<sup>33</sup> The oxidation state of a 6-P-1 phosphinidene phosphorus is I.<sup>33</sup> The oxidation state of phosphorus in 10-P-3 ADPO can also be seen to be I when

the additional lone pair of electrons at phosphorus is considered. The oxidation state of phosphorus in 10-P-3 ADPO must be reduced by 2 from the value in 8-P-3 ADPO (oxidation state III) where the phosphorus has only the single lone pair of electrons that is typically found in phosphines and phosphites.<sup>33</sup>

The P–O bond distances in 10-P-3 ADPO are only slightly longer (<6%) than the corresponding apical P–O distances in 10-P-5 centers.<sup>25</sup> This implies a significant degree of interaction between the phosphorus and oxygen centers. If 10-P-3 ADPO was really a phosphinidene center, a  $^{15}\text{N}$ – $^{31}\text{P}$  coupling constant of over 100 Hz would be observed if previously observed trends were followed.<sup>25</sup> However, the  $^{15}\text{N}$ – $^{31}\text{P}$  coupling constants are around 80 Hz (Table 2), and is generally consistent with three-coordinate phosphorus centers. Additionally, the large upfield shift of the  $^{17}\text{O}$  (>200 ppm) relative to the diketoamine starting ligand suggests a high degree of interaction between the oxygen and phosphorus centers.

### V. Calculated Geometries and Energies

The structure of the di-*tert*-butyl-ADPO and dicumyl-ADPO (Figure 2) have been determined by X-ray crystallography. The structure of the basic ADPO ring system is not particularly sensitive to substituents or crystal packing (Table 1).

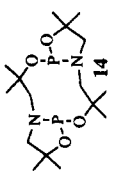
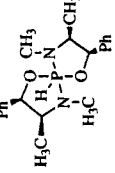
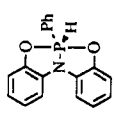
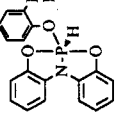
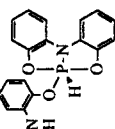
The X-ray structure of 3,7-di-*tert*-butyl-ADPO has been compared to the calculated geometry of the unsubstituted ADPO (Table 3). The calculated structure and symmetrized experimental structure ( $C_{2v}$ ) are in excellent agreement. All bond distances agree to better than 2 pm and most angles to within  $1^\circ$ . The angles at nitrogen differ by only  $0.7^\circ$  ( $\text{C–N–C}_{\text{expt}} = 124.6^\circ$ ,  $\text{C–N–C}_{\text{calc}} = 123.9^\circ$ ).

The unusual planar 10-P-3 T-shaped geometry of ADPO is one of the most interesting features of the molecule. In order to better understand this feature in contrast to the many examples of folded saturated 8-P-3 structures,<sup>21,24</sup> calculations on the folded geometry of ADPO were investigated. The energy optimized, folded  $C_s$  geometry was created by folding the two five-membered rings about the P–N bond. The results from the optimized geometry are shown in Table 3 and Figure 3.

The differences in the calculated geometry of folded ADPO ( $C_s$ ) and planar ADPO ( $C_{2v}$ ) are significant. The P–N bond distance in the folded structure is longer and the P–O bond distances are shorter. For a folded 8-P-3 structure the calculated P–O and P–N distances are expected on the basis of the covalent radii of the atoms involved. In addition, the C–O bond distances in the folded 8-P-3 structure are long compared to the calculated planar structure and are similar to normal C–O single bonds. The C–N bond lengths increase in the folded structure and the C=C bonds are shortened as a ring localized  $\pi$ -electron system develops. As expected, the bond angles change significantly between the folded and planar ADPO structures. Both the phosphorus and nitrogen are pyramidal in folded 8-P-3 ADPO.

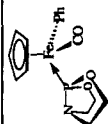
Calculations at the SCF level show that the folded 8-P-3 structure is lower in energy by 9.9 kcal/mol than the planar 10-P-3 structure. However, when electron correlation correction (MP-2) is included, the planar

Table 1. Bond Lengths (pm) and Angles (deg) of Various ADPO and Related Structures

a. ADPO and Related Nonmetallic Structures												
compound												
property	ADPO	dicumyl-ADPO	ADPO-(CH <sub>3</sub> )Cl	ADPO-(CH <sub>3</sub> ) <sub>2</sub>	ADPO-F <sub>2</sub>	ADPO-o-chloranil	ADPO-2HFB					
P-O	183.5(2)	181.3(2)	170.1(8)	174.1(8)	166.4 <sup>a</sup>	161.8(5)	170.5(6)	162.6(1) <sup>b</sup>	170.0 <sup>a</sup>	171.8 <sup>a</sup>	168.2 P-O, <sup>a</sup>	161.4 P-O, <sup>a</sup>
P-N	179.2(2)	179.5(2)	170.2(8)	173.8(8)	164.4	162.3(4)	165.6(1) <sup>c</sup>	165.6(1) <sup>c</sup>	169.0	171.5	169.6	
C-O	133.1(4)	133.7(3)	138.0(10)	137.5(4)	169.2	169.6(5)	161.3(10)	169.9(1)	143.4	136.8	136.2	
C-N	132.8(4)	133.7(3)	139.0(10)	136.8(4)	141.5	140.6(6)	140.6(10)	146.0(2) <sup>b</sup>	150.0	141.0	140.4 C-N <sup>b</sup>	
C-C	137.5(3)	138.5(3)	139.0(10)	140.9(5)	142.0	139.6(8)	140.8(10)	146.5(2) <sup>b</sup>	154.4	139.5	137.8	
O-P-O	134.2(4)	134.3(3)	135.0(2)	130.6(5)	136.5	130.5(9)	128.8(11)	153.0(2) <sup>b</sup>	176.6	165.9	168.8 <sup>b</sup>	
N-P-O	133.7(4)	134.1(3)	133.0(1)	132.5(6)	131.0	131.4(9)	176.6(5)	102.6(1)	89.2	87.8	88.4	
C-O-P	167.7(1)	167.7(2)	173.5(5)	171.7(1)	162.8	141.8(3)	88.3(3)	99.2(1) <sup>c</sup>	111.9	114.3	114.1	
C-N-P	83.5(1)	83.58(9)	87.3(6)	86.5(1)	87.3	90.8(3)	176.6(5)	116.2(1) <sup>b</sup>	115.4	115.2	114.7	
C-O-P	84.2(1)	84.22(9)	86.8(6)	86.5(1)	89.7	89.9(3)	88.3(3)	120.4(1) <sup>c</sup>	100.3	108.4	108.6	
C-N-P	114.3(2)	115.06	113.4(8)	113.1(2)	114.6	113.2(4)	113.5(6)	108.8(1) <sup>b</sup>	103.2	113.2	113.1	
C-C-O	118.0(2)	117.82	114.7(8)	113.0(3)	115.3	111.4(5)	115.5(6)	123.3(1) <sup>c</sup>	129.2	129.2	129.8	
C-C-N	116.8(2)	118.17	115.4(9)	113.3(3)	111.1	112.6(4)	129.0(10)	106.0(1) <sup>b</sup>	141.9 P-H, 141.1 P-C	141.9 P-H, 181.1 P-C	141.9 P-H, 181.1 P-C	
C-C-N	111.3(2)	109.74	111.0(10)	112.5(4)	111.1	112.1(6)	183.4(9)	115.2(1) <sup>c</sup>	108.4	108.4	108.6	
C-C-O	111.3(3)	110.98	111.0(10)	112.5(4)	111.1	111.2(6)	91.8(3)	110.2(9)	103.2	113.2	113.1	
C-C-O	112.8(2)	112.89	110.0(10)	111.6(4)	111.1	111.8(6)	91.8(3)	110.4(1) <sup>c</sup>	129.2	129.2	129.8	
C-N-C	112.3(3)	111.74	111.0(10)	117.7(3)	130.5	112.0(6)	91.8(3)	112.6(1)	141.9 P-H, 181.1 P-C	141.9 P-H, 181.1 P-C	141.9 P-H, 181.1 P-C	
C-N-C	125.2(2)	124.01	125.0(10)	127.1(3)	159.1	128.0(6)	91.8(3)	129.0(10)	108.4	108.4	108.6	
P-X			211.1(4) Cl	178.1(6)	153.2	171.7(4)	134.7(4)	183.4(9)	103.2	113.2	113.1	
X-P-O			177.0(10) CH <sub>3</sub>	179.9(5)	87.0, 87.8	163.8(5)	91.8(3)	183.4(9)	129.2	129.2	129.8	
X-P-N			92.2(3), 92.8(3) Cl	93.9(2), 93.4(2)	87.0, 87.8	87.5(2), 86.7(2)	91.8(3)	183.4(9)	141.9 P-H, 181.1 P-C	141.9 P-H, 181.1 P-C	141.9 P-H, 181.1 P-C	
X-P-N			91.4(5), 91.0(5) CH <sub>3</sub>	90.6(2), 90.2(2)	97.3, 99.8	106.8(2), 111.1(3)	91.8(3)	183.4(9)	108.4	108.4	108.6	
X-P-X			115.5(4) Cl	119.3(2)	151.8	172.0(3)	134.7(4)	183.4(9)	103.2	113.2	113.1	
X-P-X			136.6(5) CH <sub>3</sub>	128.2(2)	109.7	95.4(3)	134.7(4)	183.4(9)	103.2	113.2	113.1	
ref	20	30	25	25	30	25	25	24	31	34	26	

## b. Various ADPO Metal Complexes

compound



property	(ADPO) <sub>2</sub> PtI <sub>2</sub>	ADPO-Fe(CO) <sub>4</sub>	(ADPO) <sub>2</sub> Ag <sup>+</sup>	(ADPO) <sub>4</sub> Ni	[ADPO] <sub>2</sub> Ag <sup>+</sup> (NCCH <sub>3</sub> ) <sub>2</sub> SbF <sub>6</sub> <sup>-</sup> Li	[ADPO] <sub>2</sub> Fe(CO) <sub>3</sub>	[(ADPO) <sub>2</sub> Pt] <sup>2+</sup>	ADPO-MnCr(CO) <sub>5</sub>
P-O	161.3 <sup>a</sup>	163.5 <sup>a</sup>	180.4 <sup>a</sup>	166.3 <sup>a</sup>	177.5(12), 183.9(13)	162.8, <sup>a,b</sup> 162.1 <sup>c</sup>	159.9, <sup>a,b</sup> 158.7 <sup>c</sup>	163.8 <sup>a</sup>
P-N	170.0	170.4	172.0	177.9	172.8(14)	168.6	165.5	172.9
C-O	143.3	142.9	132.9	141.6	134.2(20), 132.2(21)	140.8, <sup>b</sup> 140.2 <sup>c</sup>	143.7, <sup>b</sup> 142.0 <sup>c</sup>	141.5
C-N	144.5	146.7	136.1	146.4	135.1(18), 129.3(21)	141.4, <sup>b</sup> 141.8 <sup>c</sup>	142.4, <sup>b</sup> 141.8 <sup>c</sup>	143.0
C-C	131.5	129.5	134.4	132.7	137.1(22), 134.7(23)	132.9, <sup>b</sup> 132.3 <sup>c</sup>	131.1, <sup>b</sup> 131.2 <sup>c</sup>	
O-P-O	113.0	108.3	167.6	110.8	167.7(6)	100.9	105.4	109.5
N-P-O	96.0	95.8	84.1	93.4	84.7(6), 83.0(6)	93.0, <sup>b</sup> 99.8 <sup>c</sup>	94.6, <sup>b</sup> 104.5 <sup>c</sup>	94.0
C-O-P	110.3	108.7	114.7	110.9	114.0(1), 115.0(1)	111.1, <sup>b</sup> 127.1 <sup>c</sup>	108.6, <sup>b</sup> 128.8 <sup>c</sup>	111.0
C-N-P	106.2	106.3	117.1	104.9	117.0(1), 117.0(1)	108.7, <sup>b</sup> 125.4 <sup>c</sup>	103.4, <sup>b</sup> 130.4 <sup>c</sup>	106.7
C-C-N	114.3	113.5	110.7	114.6	111.0(2), 115.0(2)	112.8, <sup>b</sup> 126.7 <sup>c</sup>	113.1, <sup>b</sup> 128.2 <sup>c</sup>	114.5
C-C-O	112.7	115.0	113.4	113.8	112.0(2), 111.0(2)	112.0, <sup>b</sup> 120.7 <sup>c</sup>	111.3, <sup>b</sup> 119.3 <sup>c</sup>	113.1
C-N-C	115.5	115.8	125.6	114.4	125.5(2)	120.2	120.0	116.0
P-M	220.3	215.8	261.2	209.3	243.4(6), 257.4(6)	213.3 (ax), 212.0 (eq)	229.3	212.6
P-M-P	95.8	108.5	90.00, 179.00	103.5	106.1	83.9	90.7, 165.0	
M-P-O	112.8	114.6	98.0, 89.0	113.8	94.4, 90.4, 95.1, 90.2	120.5, <sup>b</sup> 118.3 <sup>c</sup>	121.9, <sup>b</sup> 115.2 <sup>c</sup>	
M-P-O	124.4	124.6	113.3	128.4	118.3, 109.9	118.0 (ax), 121.0 (eq)	112.1	
N-P(oid)	119.0	116.5	175.0	116.8	179.0			117.0
ref	35	37	38	39	36	37	39	40

<sup>a</sup> Chemically equivalent, but crystallographically unique positions have been averaged. <sup>b</sup> Five-membered ring. <sup>c</sup> Ten-membered ring.

structure is lower in energy by 13.9 kcal/mol. This is a correlation correction of 23.8 kcal/mol. From this result it is obvious that some form of electron correlation correction is necessary for the phosphorus system to correctly model the experimental structure. Sizable correlation energy corrections in the calculation of edge inversion barriers have been noted previously.<sup>36</sup> The correlation correction is relatively small when calculating the vertex energy inversion barrier in PH<sub>3</sub> (1.3 kcal/mol out of 35.0 kcal/mol) at the MP-2 level using a DZP basis set. This correlation correction is substantially larger when calculating the edge inversion barrier for PF<sub>3</sub> (14.3 kcal/mol out of 53.8 kcal/mol) at the same level. The correlation energy corrections should be even larger for ADPO than the 14.3 kcal/mol found for PF<sub>3</sub> edge inversion because of the increase in centers in the five-membered rings over which to delocalize. It has been suggested that the chief effect of the correlation correction is to transfer electron density from the electron-rich  $\sigma$ -system (which includes the in-plane phosphorus  $\sigma$ -lone pair of electrons and the hypervalent O-P-O bond) to the out-of-plane p- $\pi$  orbital at phosphorus.<sup>14</sup> This suggestion is also consistent with the relative energetics, localization, and stabilities of the heavier congeners (As and Sb) of ADPO as discussed earlier (*vide supra*).

## VI. Edge Inversion

The ADPO molecules have served as the inspiration for the discovery of a new inversion process at main group V centers. This edge inversion process will not be fully dealt with here, but has been briefly reviewed previously.<sup>14</sup> The electronic structure shown in 7c is not expected to be the stable ground-state structure but rather is a model of a transition state for a previously unrecognized inversion process at a pnictogen center, that has been described as *edge inversion*.<sup>35</sup> The edge- and traditional vertex-inversion processes are illustrated in Figure 4. The traditional vertex-inversion process occurs by inverting a vertex and its opposite face through the center of a tetrahedron passing through a trigonal planar transition state. In contrast, the edge inversion process proceeds by the inversion of the edges of a tetrahedron through its center, thereby producing a square-planar transition state.

The various factors which favor edge or vertex inversion are summarized in Scheme 6. Although the

### Scheme 6

Vertex Inversion favored by	Edge Inversion favored by
• Electronegative Central Atom	• Electropositive Central Atom
• Electropositive Substituents	• Electronegative Substituents
• Small Central Atom	• Large Central Atom
• Large Substituents	• Small Substituents
• $\pi$ -acceptor Substituents	• $\pi$ -donor Substituents

overall outcome of the two inversion processes is the same, there are different substituent effects for the two pathways. The vertex-inversion process requires that one of the substituents (*e.g.*, the group "A" in Figure 4) pass through the center or nucleus of the tetrahedron. This is not a problem if "A" is a lone pair of electrons. However, if "A" were actually another atom, vertex inversion could not occur. Edge inversion is well suited for pyramidal three-coordinate molecules such as PF<sub>3</sub>

Table 2. Selected NMR Chemical Shifts in ADPO, ADPO-X<sub>2</sub>, and ADPO-Metal Complexes

compound	<sup>1</sup> H <sub>4(6)</sub>	<sup>13</sup> C <sub>3(7)</sub>	<sup>13</sup> C <sub>4(8)</sub>	<sup>15</sup> N <sub>5</sub>	<sup>17</sup> O <sub>2(8)</sub>	ref
di- <i>t</i> -Bu-ADPO	7.50 ( <sup>3</sup> J <sub>PH</sub> = 9.6)	169.9 (J <sub>PC</sub> = 0.2)	111.2 (J <sub>PC</sub> = 5.7)	-126.3 ( <sup>1</sup> J <sub>PN</sub> = 80.0)	324	25
diAd-ADPO	7.40 ( <sup>3</sup> J <sub>PH</sub> = 9.9)	169.6	111.1 (J <sub>PC</sub> = 5.6)	-126.0 ( <sup>1</sup> J <sub>PN</sub> = 81.0)		25
dicumyl-ADPO	7.41 ( <sup>3</sup> J <sub>PH</sub> = 9.6)	168.5	113.1 (J <sub>PC</sub> = 6.0)	-128.1 ( <sup>14</sup> N)		30
di- <i>t</i> -Bu-ADPO-F <sub>2</sub>	6.15 ( <sup>3</sup> J <sub>PH</sub> = 33.7)	148.4 (J <sub>PC</sub> = 1.2)	103.1 (J <sub>PC</sub> = 20.1)	-270.2 ( <sup>1</sup> J <sub>PN</sub> = 30.0)	151	30
di- <i>t</i> -Bu-ADPO-Cl <sub>2</sub>	6.15 ( <sup>3</sup> J <sub>PH</sub> = 35.8)	152.5 (J <sub>PC</sub> = 8.1)	102.3 (J <sub>PC</sub> = 23.0)	-262.4 ( <sup>1</sup> J <sub>PN</sub> = 13.7)	224	25
di- <i>t</i> -Bu-ADPO-Br <sub>2</sub>	6.20 ( <sup>3</sup> J <sub>PH</sub> = 35.9)	154.5 (J <sub>PC</sub> = 10.7)	102.9 (J <sub>PC</sub> = 23.3)	-256.8 ( <sup>1</sup> J <sub>PN</sub> = 6.2)		25
di- <i>t</i> -Bu-ADPO-(CH <sub>3</sub> ) <sub>2</sub> /Cl	5.99 ( <sup>3</sup> J <sub>PH</sub> = 35.6)	151.2 (J <sub>PC</sub> = 5.7)	102.0 (J <sub>PC</sub> = 13.9)	-271.0 ( <sup>1</sup> J <sub>PN</sub> = 16.9)		25
di- <i>t</i> -Bu-ADPO-(CH <sub>3</sub> ) <sub>2</sub>	5.31 ( <sup>3</sup> J <sub>PH</sub> = 31.2)	150.0 (J <sub>PC</sub> = 3.8)	99.8 (J <sub>PC</sub> = 15.5)	-303.0 ( <sup>1</sup> J <sub>PN</sub> = 17.4)	171	25
di- <i>t</i> -Bu-ADPO-H <sub>2</sub>	5.64 ( <sup>3</sup> J <sub>PH</sub> = 34.3)			-309.1 ( <sup>1</sup> J <sub>PN</sub> = 17.8)		43
{ADPO} <sub>2</sub>	5.60 ( <sup>3</sup> J <sub>PH</sub> = 5.08)					39
di- <i>t</i> -Bu-ADPO-2HFB	6.01 ( <sup>3</sup> J <sub>PH</sub> = 36.8)	141.7 (J <sub>PC</sub> = 4.9)	102.8 (J <sub>PC</sub> = 18.4)	-285.1 ( <sup>1</sup> J <sub>PN</sub> = 16.0)		25
di- <i>t</i> -Bu-ADPO-HFPO	6.24 ( <sup>3</sup> J <sub>PH</sub> = 35.4)	150.4 (J <sub>PC</sub> = 4.8)	104.1 (J <sub>PC</sub> = 19.6)	-266.8 ( <sup>1</sup> J <sub>PN</sub> = 28.2)		30
ADPO-HFBA	5.44 ( <sup>3</sup> J <sub>PH</sub> = 10.8)	210.3 (J <sub>PC</sub> = 1.1)	73.0 (J <sub>PC</sub> = 7.6)			25
ADPO-MeOH (10-P-5)	5.97 ( <sup>3</sup> J <sub>PH</sub> = 33.8)					25
ADPO-MeOH (rearranged)	5.64 ( <sup>3</sup> J <sub>PH</sub> = 6.10)					25
ADPO-HF <sub>3</sub>	6.5 ( <sup>3</sup> J <sub>PH</sub> = 23.3)			-124		25
di- <i>t</i> -Bu-ADPO- <i>o</i> -chloranil	6.25 ( <sup>3</sup> J <sub>PH</sub> = 32.0)	195.4	108.9 (J <sub>PC</sub> = 15.9)	-275.9 ( <sup>1</sup> J <sub>PN</sub> = 16.8)		25
(ADPO) <sub>2</sub> PtI <sub>2</sub>	5.95 ( <sup>3</sup> J <sub>PH</sub> = 29.0)	156.0	113.9	-276.0 ( <sup>1</sup> J <sub>PN</sub> = 44.8)		35
ADPO-Mn Cp(CO) <sub>2</sub>	5.74 ( <sup>3</sup> J <sub>PH</sub> = 24.3)	155.2 (J <sub>PC</sub> = 5.4)	113.3 (J <sub>PC</sub> = 1.1)			40
(ADPO) <sub>2</sub> Ag <sup>+</sup>	7.94 ( <sup>3</sup> J <sub>PH</sub> = 18.1)	172.7	119.4			36
(ADPO) <sub>4</sub> Ag <sup>+</sup>	7.70 ( <sup>3</sup> J <sub>PH</sub> = 14.4)	171.6	113.3 (J <sub>PC</sub> = 2.8)			38
ADPO-Cr(CO) <sub>5</sub>	5.81 ( <sup>3</sup> J <sub>PH</sub> = 24.9)	155.4 (J <sub>PC</sub> = 5.6)	113.1 (J <sub>PC</sub> = 2.0)			39
ADPO-W(CO) <sub>5</sub>	5.76 ( <sup>3</sup> J <sub>PH</sub> = 24.9)	154.8 (J <sub>PC</sub> = 5.7)	112.7 (J <sub>PC</sub> = 1.5)			39
ADPO-Fe(CO) <sub>4</sub>	5.89 ( <sup>3</sup> J <sub>PH</sub> = 26.4)	156.4 (J <sub>PC</sub> = 4.9)	113.5			37
{ADPO} <sub>2</sub> Fe(CO) <sub>3</sub>	5.58 ( <sup>3</sup> J <sub>PH</sub> = 7.4)	143.8	110.6			37
[ADPO-Ru(CH <sub>3</sub> CN) <sub>2</sub> Cp*] <sup>+</sup>	5.94 ( <sup>3</sup> J <sub>PH</sub> = 7.0)	152.9 (J <sub>PC</sub> = 6.4)	111.6 (J <sub>PC</sub> = 6.1)			
[(ADPO) <sub>2</sub> Ru(CH <sub>3</sub> CN)Cp*] <sup>+</sup>	5.79 ( <sup>3</sup> J <sub>PH</sub> = 24.1)	155.6 (J <sub>PC</sub> = 6.0)	125.2			44
(ADPO) <sub>2</sub> Ni	5.82 mult	155.9 (J <sub>PC</sub> = 2.8)	125.5			44
(ADPO) <sub>2</sub> Ni	5.4 mult	153.5	112.5			39
[{(ADPO) <sub>2</sub> ] <sub>2</sub> Pd] <sup>2+</sup>	6.15 ( <sup>3</sup> J <sub>PH</sub> = 4.7)	144.3 (J <sub>PC</sub> = 2)	111.6 (J <sub>PC</sub> = 2.4)			39
	6.31 ( <sup>3</sup> J <sub>PH</sub> = 4.6)	153.6 (J <sub>PC</sub> = 2.4)	113.0 (J <sub>PC</sub> = 1.8)			

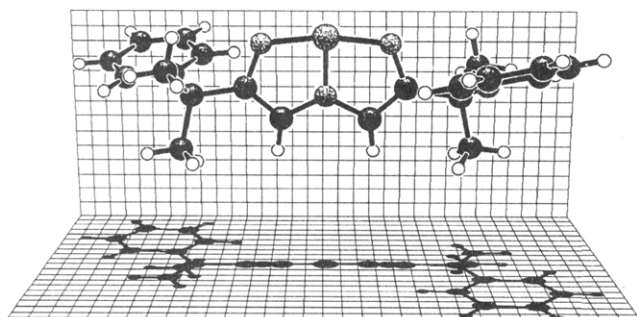
Figure 2. KANVAS<sup>42</sup> drawing of dicumyl-ADPO.<sup>30</sup>

Table 3. Calculated and Experimentally Observed Geometries for ADPO

property <sup>a</sup>	exp <sup>b</sup> planar 10-P-3	calcd <sup>c</sup> planar 10-P-3	calcd <sup>c</sup> folded 8-P-3
r <sub>P-O</sub>	180.9	180.4	165.2
r <sub>P-N</sub>	170.3	168.8	176.3
r <sub>N-C</sub>	138.3	139.4	143.8
r <sub>O-C</sub>	133.3	131.6	138.7
r <sub>C-C</sub>	134.1	134.8	132.8
θ <sub>O-P-N</sub>	83.9	83.9	92.3
θ <sub>O-P-O</sub>	167.7	167.7	108.0
θ <sub>P-N-C</sub>	117.7	118.0	107.3
θ <sub>P-O-C</sub>	115.1	115.4	112.4
θ <sub>C-N-C</sub>	124.6	123.9	112.9
θ <sub>N-C-C</sub>	110.8	109.6	113.1
θ <sub>O-C-C</sub>	112.4	113.1	114.4

<sup>a</sup> Bond distances are in picometers; bond angles, in degrees.

<sup>b</sup> Average of 3,7-di-*tert*-butylADPO and 3,7-dicumylADPO.

<sup>c</sup> Calculated geometries are for molecules in which hydrogens are used as substituents in the 3 and 7 positions.

as well as tetrahedral four-coordinate molecules like SiF<sub>4</sub> for which this process has been sometimes characterized as a twist. The edge-inversion process

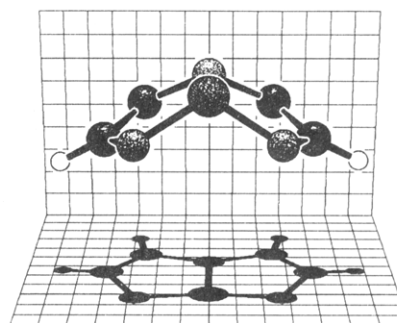
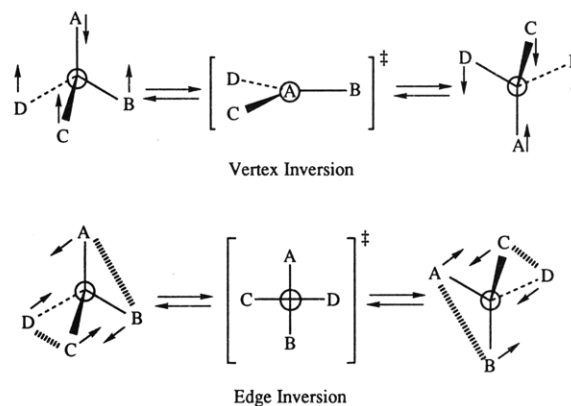
Figure 3. KANVAS<sup>42</sup> drawing of local minimum energy structure of 8-P-3 ADPO.<sup>14</sup>

Figure 4. Comparison of the vertex- and edge-inversion processes.

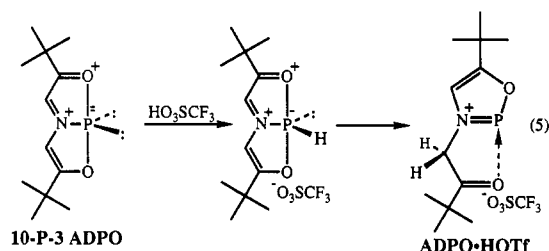
has been predicted to occur at four-coordinate tetrahedral centers.<sup>36-38</sup> Edge inversion has now been demonstrated experimentally for phosphorus,<sup>15</sup> germanium,<sup>39</sup> silicon,<sup>40</sup> bismuth,<sup>41</sup> and has recently been considered anew for carbon.<sup>36,42</sup>



## VII. Oxidative Additions of HX Compounds to ADPO

### A. Protonations of ADPO and Related Molecules

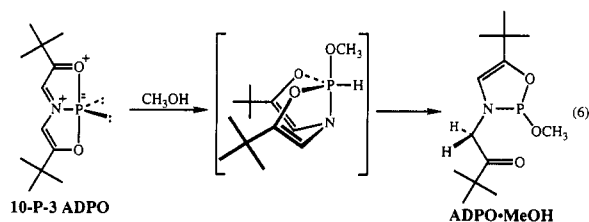
Our summary of the reactivity of low-coordinate hypervalent phosphorus compounds begins with the oxidation of hydroxylic compounds. An extreme example in this connection is the reactivity toward strong protic acids. ADPO reacts with triflic acid in  $\text{CH}_2\text{Cl}_2$  to afford a transient yellow solution that gives way to a colorless solution (eq 5).<sup>25</sup> The transient yellow



species is probably the phosphorus protonated species similar to those observed in the oxidative additions of alcohols to ADPO, *vide infra*. The NMR data of the final adduct (ADPO·HOTf) indicates the proton resides at the C4 carbon. The  $^{31}\text{P}$  NMR chemical shift at  $\delta$  234 is indicative of two-coordinate phosphorus species (Table 4).<sup>43</sup> The  $^{15}\text{N}$  NMR chemical shift at  $\delta$  -153 is compatible with an increase in electron density, but not as much as the pyramidal nitrogen in the 8-P-4 complexes of ADPO (*vide infra*).

The methylene resonance at  $\delta$  5.84 ( $^3J_{\text{PH}} = 7.8$  Hz) and the vinyl proton at 7.81 ( $^3J_{\text{PH}} = 6.4$  Hz) is consistent with the proposed ADPO·HOTf structure. There appears to be an interaction between the phosphorus center and the carbonyl oxygen as evidenced by the vicinal coupling between the vinyl proton and the methylene carbon which requires an antiperiplanar arrangement for these atoms. Further evidence for the phosphorus–oxygen interaction is seen in the  $^{13}\text{C}$  NMR where the two carbons attached to the oxygens exhibit the following chemical shifts and phosphorus coupling constants:  $\delta$  215.8 ( $J_{\text{PC}} = 3.17$  Hz) and 171.2 ( $J_{\text{PC}} = 3.36$  Hz). IR spectroscopy also supports this phosphorus–oxygen interaction with an absorption at 1695  $\text{cm}^{-1}$  for the “free” carbonyl (carbonyl absorption for the diketoamine ligand =  $\sim 1710$   $\text{cm}^{-1}$ ).<sup>44</sup> The dioxachalcapentalenes exhibit similar regiochemistry upon protonation.<sup>45</sup>

The reaction of ADPO with  $\text{CH}_3\text{OH}$ ,  $(\text{CH}_3)_2\text{CHOH}$ , or *p*-cresol gives rapid oxidative addition of the alcohol to afford the transient bicyclic phosphorane (eq 6).<sup>25</sup>

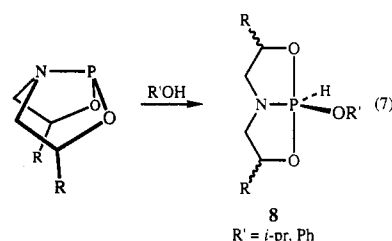


This species has been identified in the  $^1\text{H}$  and  $^{31}\text{P}$  NMR. The proton is directly attached to the phosphorus to produce 10-P-5 ADPO·MeOH initially. Over time the 10-P-5 ADPO·MeOH bicyclic phosphorane rearranges

to a three-coordinate phosphorus species, 8-P-3 ADPO·MeOH.

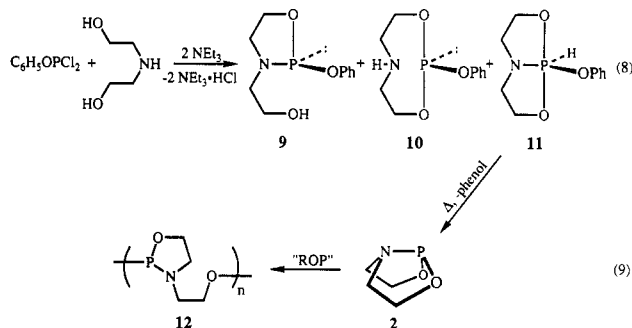
The 10-P-5 ADPO·MeOH chemical shift is also comparable to a benzo-fused 10-P-5 bicyclic phosphorane (4) prepared by Contreras. The proton directly bound to phosphorus exhibits a chemical shift of 8.00 ppm while the phosphorus center resonates at  $\delta$  -35 ( $J_{\text{PH}} = 898$  Hz)<sup>26</sup> (Table 4). Because of substitution (benzo fusion in the ring backbone) or saturation of the ligand backbone, the bicyclic phosphoranes of Contreras and Wolf do not rearrange to the 8-P-3 phospholane species.

These protonations and oxidative additions can be compared with the compounds of Wolf and co-workers in which saturated analogs of ADPO are reacted with alcohols or amines (eq 7).<sup>23</sup> These additions appear to



proceed smoothly to give the bicyclic phosphoranes (8) which are reported to be stable. The  $^{31}\text{P}$  NMR shifts and  $J_{\text{PH}}$  coupling constants indicate that the proton is directly bound to the phosphorus.

Another interesting type of oxidative addition reported by Wolf is found in the following reactions (eqs 8 and 9).<sup>22</sup>



When  $\text{C}_6\text{H}_5\text{OPCl}_2$  reacted with diethanolamine in the presence of  $\text{NEt}_3$  they detected three products (9, 10, and 11) in the  $^{31}\text{P}$  NMR. An equilibrium among 9, 10, and 11 may involve reversible oxidative addition of O–H bonds to the 8-P-3 phosphorus center. Over time oxazaphosphorane 9 concentration decreased with a concomitant increase in the phosphorane 11 concentration but there was no change in the concentration of 10. Increasing the temperature caused a reductive elimination of phenol from 11 leading to the formation of 2. However, 2 underwent a facile ring opening polymerization (ROP) to give 12.

A stable bicyclic phosphane 13 has been prepared from 4,4,6,6-tetramethyl-3-azapentane-1,5-diol and tris(dimethylamino)phosphane (eq 10).<sup>24</sup> The reaction

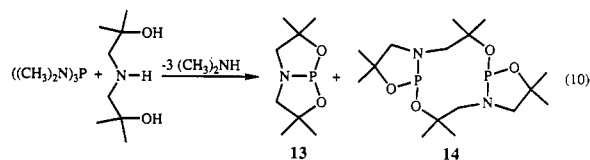


Table 4. Various  $^{31}\text{P}$  Chemical Shifts (ppm  $\delta$ )

Compound	$^{31}\text{P}$ Shift	ref	Compound	$^{31}\text{P}$ Shift	ref
	264	56		160.8	57
ADPO•MnCp(CO) <sub>2</sub>	256	40		159.0	25
ADPO•Fe(CO) <sub>4</sub>	235	37		152	36
	234.2	25		(broad singlet)	
ADPO•Cr(CO) <sub>5</sub>	231	39		147.7	21
[(ADPO) <sub>2</sub> •Ru(CH <sub>3</sub> CN)Cp*] <sup>+</sup> -O <sub>3</sub> SCF <sub>3</sub>	201	44		145.1	22
(ADPO) <sub>4</sub> Ni	200	39		144.6, 152	23
[ADPO•Ru(CH <sub>3</sub> CN) <sub>2</sub> Cp*] <sup>+</sup> -O <sub>3</sub> SCF <sub>3</sub>	198	44		140	24
	188.3	30		139.6	23
	187	25		133.9	39
ADPO	185.0	25		133.6	22
ADPO•W(CO) <sub>5</sub>	180	39		126.5	35
	( <i>J</i> <sub>PW</sub> = 398 Hz)			122.4	25
{ADPO} <sub>2</sub> •Fe(CO) <sub>3</sub>	172	37		90.3	39
(ADPO) <sub>4</sub> Ag <sup>+</sup> SbF <sub>6</sub> <sup>-</sup>	166	38		-0.8	25
	(broad singlet)			-3.9, -4.2	23
	163.6	25			
	163	24			
	162	57			

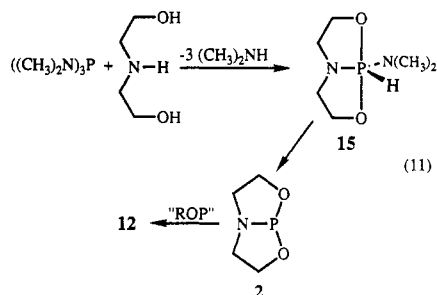
Table 4 (Continued)

Compound	$^{31}\text{P}$ Shift	ref	Compound	$^{31}\text{P}$ Shift	ref
	-9.1	25		-40 ( $J_{\text{PH}} = 820$ Hz)	23
	-10.2	25		-41.4 ( $J_{\text{PH}} = 820$ Hz)	21
	-21.8	25		-41.6 ( $J_{\text{PH}} = 854$ Hz)	26
	-24.9	25		-41.7 ( $J_{\text{PH}} = 820$ Hz)	23
	-32.6 ( $^1J_{\text{PF}} = 1021$ Hz, $^2J_{\text{PF}} = 79.5$ Hz)	30		-43.1 ( $^1J_{\text{PH}} = 672$ Hz, $^3J_{\text{PH}} = 34$ Hz)	43
	-34.0 ( $J_{\text{PF}} = 875.5$ Hz)	30		-49.3 ( $J_{\text{PH}} = 709$ Hz)	26
	-34.4	25		-61.8 ( $J_{\text{PH}} = 655$ Hz)	58
	-35.0 ( $J_{\text{PH}} = 898$ Hz)	26		-84	59
	-38.3 ( $J_{\text{PH}} = 830$ Hz)	23		-90	22
	-38.5 ( $J_{\text{PH}} = 826$ Hz)	23		-90.7	25
				-112.8	25

mixture exhibits two peaks in the  $^{31}\text{P}$  NMR, 163 and 140 ppm, which can be attributed to the phosphane and dimer, respectively. The phosphane can be distilled from the dimer (which is a solid) under high vacuum

at 29 °C. This dimer is very similar to the ADPO dimer, which will be discussed below. However, unlike Wolf's dimer, the ADPO dimer readily reverts to ADPO at room temperature.

Wolf described the transformation of tricovalent to pentacovalent phosphorus centers (8-P-3  $\rightarrow$  10-P-5) by controlled oxidative addition.<sup>22</sup> In an attempt to prepare the bicyclic phosphane **2** using  $(\text{Me}_2\text{N})_3\text{P}$  and diethanolamine they encountered an immediate oxidative addition reaction between dimethylamine and the 8-P-3 bicyclic phosphane to give the 10-P-5 bicyclic phosphorane **15** (eq 11). This is a reversible process

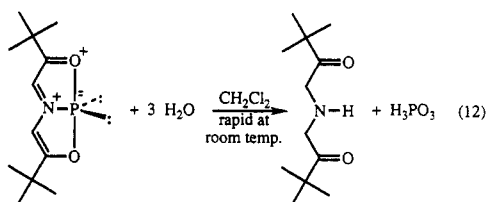


and the 10-P-5 bicyclic phosphorane eliminates dimethylamine to give the 8-P-3 bicyclic phosphane **2**, which then polymerizes, **12**.

On the basis of  $^1\text{H}$  and  $^{31}\text{P}$  NMR the chemistry and structures of the 10-P-5 compounds of Wolf and Contreras (in most cases) are similar to the ADPO-ROH (R = Me, *i*Pr, and *p*-cresol) adducts. However, oxidative addition of secondary amines to 10-P-3 ADPO has not been observed. The redox capability in the ADPO backbone, which is very important in determining the geometry and electron distribution in the three-coordinate phosphorus compounds, does not participate in this fashion when five-coordinate phosphorus centers form by oxidative addition.

## B. Hydrolysis of ADPO

ADPO will rapidly hydrolyze in moist  $\text{CH}_2\text{Cl}_2$  in a matter of minutes at room temperature to give the phosphorus acid salt of the diketo amine ligand (eq 12).<sup>25</sup>

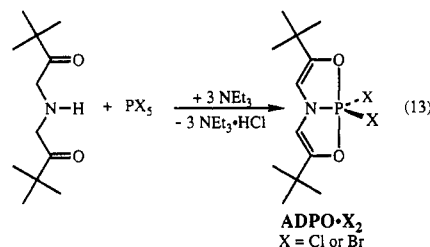


In contrast, arsenic analog ADAsO, can be recovered after 2 days (> 90%) under the same conditions. However, very prolonged exposure did lead to decomposition of the compound. ADSbO can be hydrolyzed in moist  $\text{CH}_2\text{Cl}_2$  at room temperature over 2 days to give the diketo amine and  $\text{Sb}_2\text{O}_3$ .<sup>25</sup>

## C. Oxidative Additions of Halogens

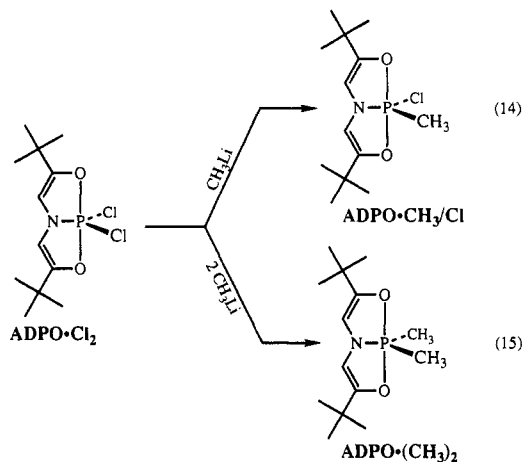
The 10-P-5 ADPO- $\text{X}_2$  adducts can be prepared by the oxidative addition of  $\text{X}_2$  to ADPO.<sup>25</sup> These halogen bonds can be formed at the phosphorus center via the use of the halogenation reagents,  $\text{PX}_5$ ,  $\text{X}_2$ , and  $\text{SO}_2\text{Cl}_2$ . Alternatively, 10-P-5 ADPO- $\text{X}_2$  can be prepared by the direct introduction of  $\text{PX}_5$  into the diketo amine ligand **3**; this is the method of choice for preparing these 10-

P-5 ADPO- $\text{X}_2$  compounds. ADPO- $\text{Cl}_2$  and ADPO- $\text{Br}_2$  can be prepared in good yield by the addition of  $\text{PCl}_5$  or  $\text{PBr}_5$  to the diketo amine (eq 13).



Solid-state structures of ADPO- $\text{Cl}_2$  or ADPO- $\text{Br}_2$  have not been determined. However, multinuclear magnetic resonance data ( $^1\text{H}$ ,  $^{13}\text{C}$ ,  $^{15}\text{N}$ ,  $^{31}\text{P}$ ) are consistent with the 10-P-5 system. The  $^{31}\text{P}$  chemical shift for the ADPO- $\text{Cl}_2$  is  $-24.9$  ppm, which is comparable to other 10-P-5 compounds reported by Wolf (Table 4). The ring proton resonance of 6.15 ppm and  $^3J_{\text{PH}} = 36$  Hz, along with the  $^{15}\text{N}$  chemical shift of  $-262$  ppm ( $^1J_{\text{PN}} = 14$  Hz) is indicative of a neutral, essentially planar ligand backbone. These data again indicate that the redox properties of the ADPO ligand backbone do not lead to electron transfer to five-coordinate phosphorus centers as occurs in the three-coordinate compounds.

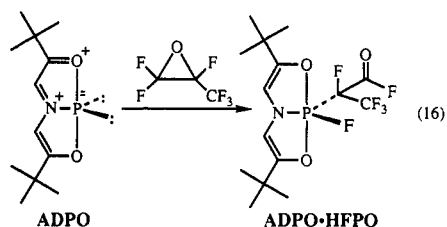
The ADPO- $\text{Cl}_2$  complex can be alkylated with 1 or 2 equiv of  $\text{CH}_3\text{Li}$  to produce ADPO- $\text{CH}_3/\text{Cl}$  and ADPO- $(\text{CH}_3)_2$  respectively (eqs 14 and 15).<sup>25</sup> Both of these compounds show solution NMR spectra similar to ADPO- $\text{Cl}_2$ .



ADPO- $\text{CH}_3/\text{Cl}$  and ADPO- $(\text{CH}_3)_2$  are well behaved, crystalline materials and their solid-state structures have been determined by single-crystal X-ray diffraction studies.<sup>25</sup> Both compounds exhibit essentially *tbp* geometries about the phosphorus 10-P-5 center, but the ADPO- $\text{CH}_3/\text{Cl}$  complex tends toward a distorted square pyramid. In both systems the ligand ring system adopts a nonplanar configuration and the nitrogen is slightly pyramidal. A shortening of the P-O bonds, compared to *di-tert*-butyl-ADPO and *dicumyl*-ADPO, also is observed in these 10-P-5 species (Table 1). There is a somewhat asymmetric geometry that is not unusual for other 10-P-5 systems that incorporate a tridentate ligand substituted in the 3 and 4 positions or benzofused at positions 6 and 7.<sup>46</sup>

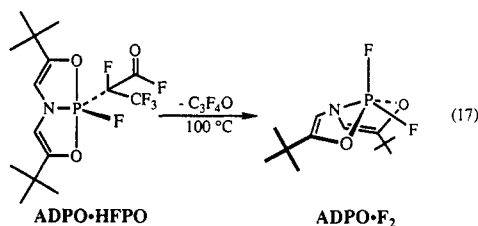
The 10-P-3 ADPO (di-*tert*-butyl and dicumyl) molecules have an average P–O bond distance of  $\sim 181$  pm (Table 3), while the 10-P-5 ADPO·CH<sub>3</sub>/Cl and ADPO·(CH<sub>3</sub>)<sub>2</sub> exhibit average P–O bond distances of  $\sim 170$  and  $\sim 174$  pm respectively. The shortening of the P–O bond in going from a 10-P-3 to a 10-P-5 species is expected on the basis of the higher oxidation state of phosphorus and may also reflect the elimination of lone pair electron repulsion between the phosphorus and oxygen centers.<sup>30</sup>

ADPO·F<sub>2</sub> was the last in the 10-P-5 ADPO·X<sub>2</sub> series to be prepared. This adduct was formed<sup>30</sup> by an indirect route discovered during the investigation of the reaction chemistry of ADPO with fluorocarbons. When ADPO reacts with hexafluoropropylene oxide at room temperature, a 1:1 adduct is formed (eq 16).



The <sup>31</sup>P NMR spectra is consistent with a 10-P-5 system,  $\delta -32.6$ , and is similar to shifts of the other ADPO·X<sub>2</sub> adducts, ADPO·Cl<sub>2</sub>, ADPO·CH<sub>3</sub>/Cl, and ADPO·(CH<sub>3</sub>)<sub>2</sub>. A large P–F coupling constant of 1021.1 Hz is indicative of a fluorine directly attached to the phosphorus. The upfield shift of the ring proton,  $\delta 6.24$  (<sup>3</sup>J<sub>PH</sub> = 35.4 Hz), and the <sup>15</sup>N shift of  $\delta -266.8$  (<sup>1</sup>J<sub>PN</sub> = 28.2 Hz) are concordant with the reduction of the ligand ring system. Unfortunately the structure of ADPO·HFPO could not be completely determined because of disorder in the fluoroalkyl group. However, partial refinement of the atoms in the ligand backbone and the phosphorus atom yielded atomic positions similar to the ADPO·CH<sub>3</sub>/Cl and ADPO·(CH<sub>3</sub>)<sub>2</sub> structures.

When ADPO·HFPO is heated to 100 °C, an unidentified fluorocarbon fragment is eliminated and a new P–F bond is formed to give ADPO·F<sub>2</sub> (eq 17). No ADPO



can be isolated or detected in the reaction media, indicating that HFPO has served as an F<sub>2</sub> donor. Multinuclear magnetic resonance indicates a 10-P-5 ADPO·F<sub>2</sub> species. The <sup>31</sup>P resonance of  $-34.0$  ppm is a triplet due to coupling of the two fluorine atoms. As in the precursor ADPO·HFPO and the other 10-P-5 ADPO·X<sub>2</sub> complexes, the ring protons shift upfield ( $\delta 6.15$ ) and a large coupling constant is observed (<sup>3</sup>J<sub>PH</sub> = 33.7 Hz). The <sup>15</sup>N resonance at  $-270.2$  ppm (<sup>1</sup>J<sub>PN</sub> = 30.0 Hz) is also indicative of a reduced positive charge in the tridentate ligand.

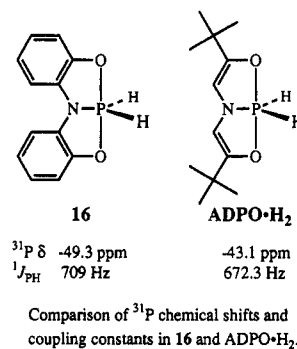
The solid-state structure of ADPO·F<sub>2</sub> was determined by single-crystal X-ray diffraction. While ADPO·CH<sub>3</sub>/

Cl and ADPO·(CH<sub>3</sub>)<sub>2</sub> tend to be essentially t<sub>bp</sub>, ADPO·F<sub>2</sub> deviates dramatically from the idealized t<sub>bp</sub> geometry. In fact, ADPO·F<sub>2</sub> exhibits the “strainless” square-pyramidal geometry described by Holmes and co-workers.<sup>47,48</sup>

In the ADPO·F<sub>2</sub> structure, the P–O bonds (average = 165.4 pm) are even shorter than those observed in the other ADPO·X<sub>2</sub> adducts. These P–O bond distances are similar in length to the ADPO·*o*-chloranil adduct (*vide infra*). These short P–O bond distances are probably a consequence of the highly distorted t<sub>bp</sub> geometry.

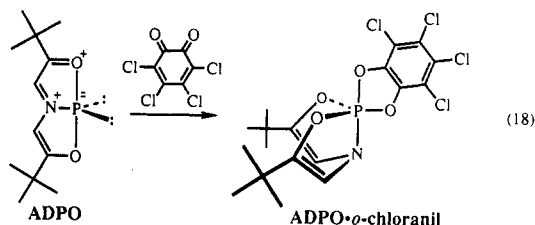
Although not a halogen, hydrogen (H<sub>2</sub>) addition to the phosphorus center of ADPO would lead to a related bis(P–H) phosphorane. ADPO·H<sub>2</sub> can be prepared from the reduction of ADPO·Cl<sub>2</sub> with LiAlH<sub>4</sub>.<sup>49</sup> However, it is unstable and slowly decomposes with reductive elimination to give ADPO. The multinuclear magnetic resonance spectra are consistent with the proposed structure. The proton-coupled <sup>31</sup>P spectra exhibits a triplet of triplets at  $-43.1$  ppm (<sup>1</sup>J<sub>PH</sub> = 672.3 Hz, <sup>3</sup>J<sub>PH</sub> = 34.33 Hz). This <sup>31</sup>P shift is similar to the dihydrobenzo-fused bicyclic phosphorane reported by Contreras (Scheme 7).<sup>26</sup>

#### Scheme 7



#### D. Reactions of ADPO with Dicarbonyl Compounds

ADPO will react smoothly with *o*-chloranil to yield a 10-P-5 ADPO·*o*-chloranil species, (eq 18).<sup>25</sup> The



phosphorus atom of the adduct retains its 10-electron count upon formation of the two new P–O bonds to the *o*-chloranil oxygens even though two electrons are returned to the ligand backbone. The return of two electrons to the ligand ring system causes the nitrogen atom to become pyramidal, which in turn causes a folding of the two five-membered rings. The angle between the two rings becomes 146°. The <sup>15</sup>N NMR chemical shift of  $-275.9$  ppm (<sup>1</sup>J<sub>PN</sub> = 16.8 Hz) is in agreement with other pyramidal 8-N-3 species.<sup>28,50</sup>

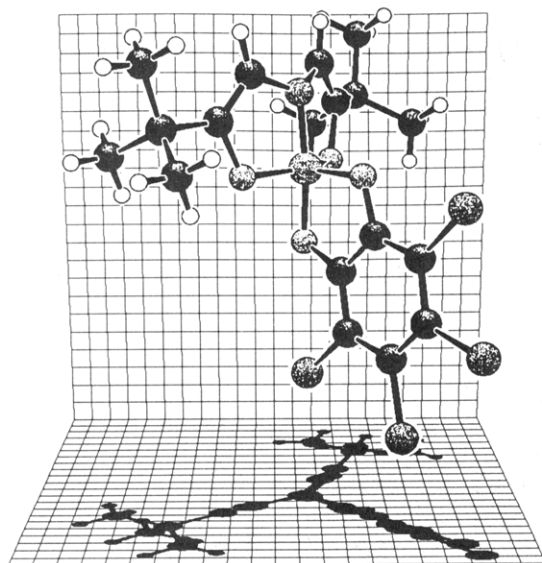
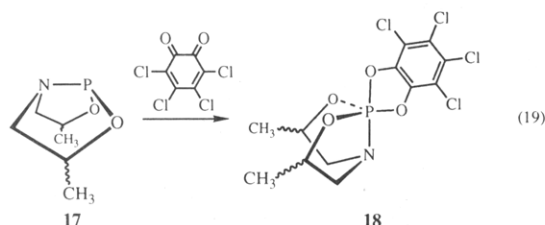


Figure 5. KANVAS<sup>42</sup> Drawing of ADPO-*o*-chloranil adduct.

There are other reports of similar 10-P-5 adducts of *o*-chloranil by Wolf and co-workers (eq 19).<sup>23</sup> In these

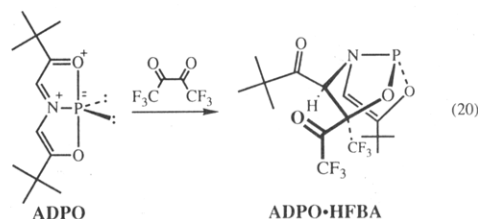


cases an 8-P-3 bicyclic phosphane 17 reacts with *o*-chloranil to form the 10-P-5 species 18 shown in eq 19. Due to the 3,7-dimethyl substitution in the ring, two diastereomers are formed, which produce two signals in the <sup>31</sup>P NMR. The <sup>31</sup>P chemical shift of ADPO-*o*-chloranil adduct (<sup>31</sup>P δ -10.2) is similar to those adducts observed by Wolf *et al.* for 18 (<sup>31</sup>P δ -3.9 and -4.2). These <sup>31</sup>P shifts are consistent with 10-P-5 centers.

The geometrical arrangements of the atoms about the phosphorus atom in the 10-P-5 ADPO-*o*-chloranil adduct is not a perfectly idealized 10-P-5 tbp geometry. It is midway between the tbp and square-pyramidal structures (Figure 5). The best tbp structure places the nitrogen atom and one oxygen atom of the *o*-chloranil moiety at the apical positions. The closest fit to a square-pyramidal geometry places the nitrogen and the two oxygen atoms from the original ligand, and one oxygen atom from the *o*-chloranil ligand in the basal plane. The O-P-O angle in the eight-membered ring of the ADPO-*o*-chloranil adduct is 141.8°. A 172.0° N-P-O angle is found between the tbp apical positions. The distorted geometry is between tbp structures found for ADPO·(CH<sub>3</sub>)<sub>2</sub>, ADPO·CH<sub>3</sub>/Cl and ADPO·2HFB (*vide infra*) and square pyramidal geometry found for ADPO·F<sub>2</sub>.

Hexafluorobiacetyl (HFBA) does not follow the same reactivity pattern as *o*-chloranil upon reaction with ADPO (eq 20).<sup>25</sup> Only one of the carbonyl groups of HFBA is involved. This carbonyl group adds across the phosphorus and C4 (the carbon atom attached to the nitrogen) positions. The result is the breaking of

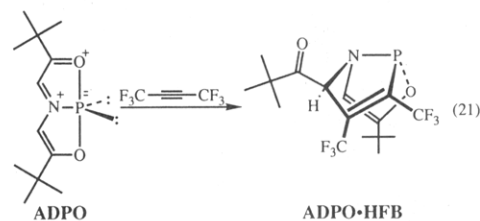
one of the original phosphorus oxygen bonds and the formation of a new, saturated five-membered ring.



The solid-state structure of the adduct has the pivaloyl and trifluoroacetyl groups on the exo face of the saturated five-membered ring of a folded bicyclic geometry. The <sup>31</sup>P resonance shifts upfield to δ 159 which is comparable to the completely saturated analogs 2 and 13 (Table 4) as well as the ADPO-hexafluoro-2-butyne adduct discussed later.

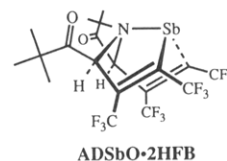
### E. Reactions of ADPO with Hexafluoro-2-butyne

Hexafluoro-2-butyne (HFB) is clearly not an α-dicarbonyl compound; however, it does show reactivity toward ADPO which is reminiscent of both *o*-chloranil and hexafluorobiacetyl. One equivalent of HFB reacts with ADPO to give an adduct with a structure similar to ADPO·HFBA (eq 21).<sup>25</sup> The carbon-carbon triple



bond of the hexafluoro-2-butyne adds across the phosphorus and C4 (carbon atom attached to the nitrogen) to form a new five-membered ring while breaking the P-O bond.

As in the ADPO·HFBA adduct, the pivaloyl group is on the exo face of the new five-membered ring. The bicyclic ring structure of ADPO·HFB is strongly folded which is not particularly surprising since a planar structure would have placed a carbon in an apical position at a ψ-tbp phosphorus center. The <sup>31</sup>P NMR spectrum shows resonances at δ 163.6, which is similar to the ADPO·HFBA adduct. The solution spectra <sup>1</sup>H, <sup>13</sup>C, <sup>15</sup>N, and <sup>19</sup>F are also consistent with the solid-state structure. By contrast, at -78 °C ADSbO reacts rapidly with HFB to give a 1:2 adduct (ADSbO·2HFB).<sup>25</sup> (The 1:1 adduct has not been observed.) The ADSbO·2HFB adduct possesses two new rings, with each ring analogous to the ADPO·HFB adduct.



At 105 °C a second mole of HFB can be added to ADPO·HFB to give an interesting λ<sup>5</sup>-phosphole (10-P-5) ADPO·2HFB complex (eq 22). The solution NMR

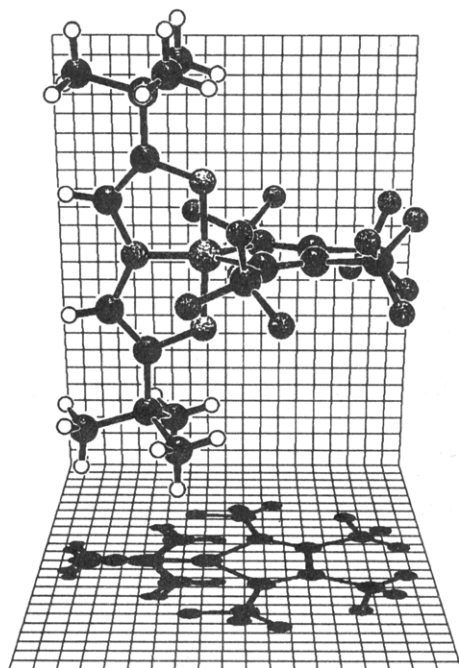
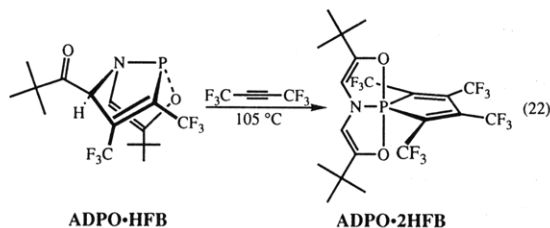


Figure 6. KANVAS<sup>42</sup> Drawing of ADPO·2HFB.<sup>25</sup>

(<sup>1</sup>H, <sup>13</sup>C, <sup>15</sup>N, <sup>19</sup>F, <sup>31</sup>P) are indicative of two planar orthogonal ring systems for the ADPO·2HFB adduct.

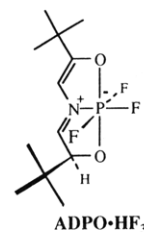


The structure of ADPO·2HFB was also verified by single-crystal X-ray diffraction analysis (Figure 6). For this complex to be formed, a major geometrical rearrangement is required to go from ADPO·HFB to a 10-P-5 ADPO·2HFB complex. This stepwise rearrangement was speculated to occur by P–O bond cleavage from the assistance of the nitrogen lone pair to form an 8-P-2 phosphide and iminium center. The second mole of HFB would add via a 2 + 3 cycloaddition across the  $\pi$ -system of the initial HFB unit and the phosphide center. The next step was postulated to be carbon-carbon bond cleavage and then reestablishment of the two P–O bonds to form the 10-P-5 ADPO·2HFB species. Special mention should be made of the blue color of ADPO·2HFB. In general,  $\lambda^5$ -phospholes which bear conjugating substituents are yellow<sup>51</sup> to orange.<sup>52</sup> However, ADPO·2HFB is bis-*ipso*-aromatic<sup>53</sup> and could be spiroconjugated.<sup>54,55</sup>

### F. Six-Coordinate Phosphorus System

ADPO·Cl<sub>2</sub> reacts with tris(dimethylamido)sulfonium difluorotrimethylsilicate (TASF) to substitute the chlorides for fluorides. However, in the presence of tris(dimethylamido)sulfonium difluoride (TAS<sup>+</sup>FHF<sup>-</sup>), HF will quickly add to ADPO·F<sub>2</sub> to give hexacoordinate ADPO·HF<sub>3</sub>. This results in another fluoride attaching to the phosphorus center and protonation of the *tert*-butyl bearing carbon. The <sup>31</sup>P NMR suggests a six-

coordinate phosphorus center ( $\delta$  -113). The fact that the <sup>14</sup>N resonance can be observed at  $\delta$  -123 is consistent with a positively charged, planar nitrogen. Finally, the <sup>31</sup>P–<sup>15</sup>N coupling constant of <1 Hz is in line with our observations of a decrease in P–N coupling constant with an increase in phosphorus coordination number.<sup>26</sup>



### VIII. Nuclear Magnetic Resonance Spectra

The primary tool for determining the geometry of the reaction products from ADPO chemistry has been <sup>31</sup>P NMR. There are a number of important factors that contribute to <sup>31</sup>P chemical shifts: coordination number, neighboring groups ( $\sigma$ - and  $\pi$ -effects), and paramagnetic contributions. In the absence of transition metals the most important factor is coordination number at phosphorus. The phosphorus chemical shifts in Table 4 have been arranged in descending order. The relation to coordination number is readily apparent. The reaction of ADPO with triflic acid goes through a yellow intermediate with the final product being the two-coordinate ADPO·HOTf, which exhibits a <sup>31</sup>P chemical shift at 234.2 ppm. This chemical shift is comparable to the dicoordinate, five-membered ring, phosphonium reported by Huttner and co-workers at 264 ppm (Table 4).<sup>56</sup> As the coordination number at phosphorus increases to three, as in any of the bicyclic phospholanes of Wolf or the 10-P-3 ADPO compounds (dicumyl-ADPO, di-*tert*-butyl-ADPO, and diadamantyl-ADPO) the <sup>31</sup>P chemical shifts move upfield. The phosphorus chemical shifts move further upfield as the coordination number increases to five (<sup>31</sup>P chemical shift ranges  $\sim 0 \rightarrow -62$  ppm) for ADPO·Cl/CH<sub>3</sub> to the saturated ADPO·H<sub>2</sub> analog of Wolf<sup>57</sup> or the benzo-fused 10-P-5 compounds of Contreras (Table 4).<sup>26</sup> Finally, six-coordinate phosphorus centers exhibit the greatest upfield shifts in this series. The ADPO·HF<sub>3</sub> shows an upfield shift of -112.4 ppm, which is comparable to other six-coordinate phosphorus centers reported by Wolf.<sup>22,58</sup>

The high dispersivity of the <sup>13</sup>C, <sup>15</sup>N, and <sup>17</sup>O nuclei also have greatly facilitated the characterization of ADPO-derived systems. There is about a 150-ppm upfield shift in the <sup>17</sup>O resonances of the ADPO backbone as a folded (reduced) ligand structure is formed from the initial 10-P-3 ADPO planar (oxidized) ligand.<sup>30</sup> The <sup>15</sup>N NMR likewise undergoes a substantial upfield shift ( $\sim 150$  ppm) as the folded amine structure is attained from the initial iminium center in 10-P-3 ADPO.<sup>26</sup> Interestingly, the simple observation of an <sup>14</sup>N resonance usually indicates a planar ligand geometry since the less symmetric folded structures generally preclude observation of the <sup>14</sup>N nucleus as a result of the extreme line width.<sup>25</sup> An interesting general trend in <sup>15</sup>N–<sup>31</sup>P coupling constants with phosphorus coordination number has also been noted for ADPO derived compounds.<sup>25</sup> The most sensitive carbon nucleus in

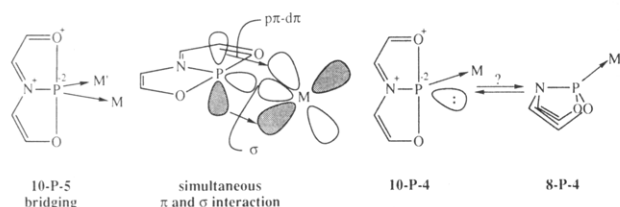
the ligand backbone is the carbon attached to oxygen which resonates at about 20 ppm higher field in the folded (ligand-reduced) structures than in the planar (oxidized ligand) structures.

Although the  $^1\text{H}$  NMR does not have the dramatic shift differences observed with the heavier nuclei, the resonance of the ligand ring proton does experience a convenient and reliable shift of 1.5–2.0 ppm upfield as a reduced ligand structure is formed from an oxidized ligand structure.<sup>25</sup> The phosphorus–proton coupling constant ( $^3J_{\text{HP}}$ ) to the ring proton is also a useful indicator of the presence or absence of lone pair electrons at phosphorus and thereby the oxidation state of the ligand backbone.<sup>25</sup>

### IX. Transition Metal Complexes

The coordination chemistry of 8-P-3 (phosphine) compounds with transition metal centers is a widely recognized and extensively studied area of coordination chemistry. Since 10-P-3 ADPO possesses two lone pairs of electrons at a single phosphorus center, there is an opportunity to observe unique phosphorus-bridged metal systems with a 10-P-5 center acting as the bridging ligand. It is also conceptually possible that the phosphorous center of 10-P-3 ADPO could serve as both a  $\sigma$ - and  $\pi$ -donor to a single transition metal center, a feat not possible for the common three-coordinate eight-electron phosphorus donors (phosphines). A third opportunity arises from an interplay of the 10-P-3  $\leftrightarrow$  8-P-3 electromorphism possible in the ADPO molecules with chemistry at the metal center so that either a 10-P-4 or 8-P-4 arrangement (or both) could form. This latter opportunity has been realized in the transition metal coordination chemistry of ADPO, and there are now compounds which clearly demonstrate the bridging ligand capability and suggest a role for a  $\sigma$ - $\pi$  double interaction with a single metal center. These various coordination modes are illustrated in Scheme 8. We

Scheme 8

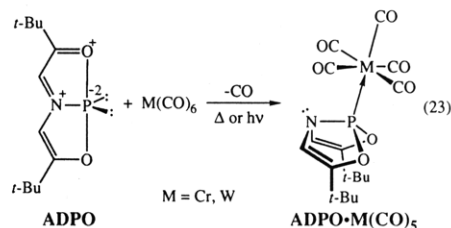


will present the transition metal chemistry of ADPO not in chronological order of discovery but rather from left to right through the transition series making note of the various coordination modes.

#### A. Complexes with the Transition Group 6 Metals, Cr and W

Both chromium and tungsten hexacarbonyls form 1:1 adducts with ADPO, and in both cases the ADPO molecule adopts the folded, 8-P-4 structure (eq 23).<sup>59</sup>

The ring proton of the ligand backbone shifts upfield from  $\delta$  7.5 in uncomplexed ADPO to  $\delta$  5.81 ( $^3J_{\text{PH}} = 24.9$  Hz) for ADPO·Cr(CO)<sub>5</sub> and  $\delta$  5.76 ( $^3J_{\text{PH}} = 24.9$  Hz) for ADPO·W(CO)<sub>5</sub>. The carbons in the 3 and 7 positions (attached to oxygen) of the ADPO ring are shifted upfield by 14.5 ppm in the case of the chromium

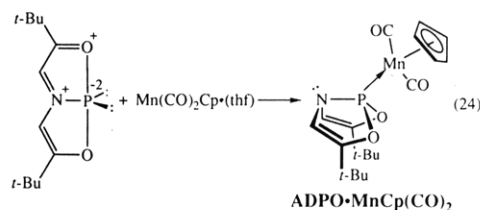


compound and 15.1 ppm for the tungsten adduct. The  $^{31}\text{P}$  NMR chemical shifts are different for the chromium and tungsten compounds ( $\delta$  231 for ADPO·Cr(CO)<sub>5</sub> and  $\delta$  180 for ADPO·W(CO)<sub>5</sub>) and actually bracket the value of 187 observed for uncomplexed 10-P-3 ADPO. Although the  $^{31}\text{P}$  shifts do not provide any structurally meaningful information in the case of these transition metal adducts, the  $^1\text{H}$  and  $^{13}\text{C}$  shifts and the  $^3J_{\text{HP}}$  coupling constants are diagnostic of the geometric and electronic changes occurring in the ADPO fragment.<sup>25,60</sup> The large increase in the  $^3J_{\text{HP}}$  coupling constant from the value of 9.6 Hz in 10-P-3 ADPO is attributed to an increase in s-orbital participation in bonding at phosphorus as a result of the loss of lone pairs of electrons. This correlation between  $^3J_{\text{HP}}$  and phosphorus oxidation state was noted above in regard to the oxidative additions to the phosphorus(I) center in 10-P-3 ADPO which yielded phosphorus(V) adducts.<sup>25</sup> A similar relationship has been observed for  $^3J_{\text{HSn}}$  coupling constants for systems in which a tin center replaces the phosphorus center in ADPO.<sup>61</sup> The upfield shift in the resonances for H<sub>4(6)}</sub> and C<sub>3(7)}</sub> reflect the increase and localization in  $\pi$ -electron density in the organic ligand backbone of ADPO. In some cases this electron density increase leads to a folding of ADPO ring system (such as metal complexes involving a four-coordinate phosphorus center, *vide infra*).<sup>59,60,62,63</sup> In other cases the geometry of the phosphorus centers requires that the organic ligand backbone remain essentially planar in spite of the localization and electron density increase, forcing a planar distorted organic ligand backbone (e.g. ADPO·(CH<sub>3</sub>)<sub>2</sub> and ADPO·CH<sub>3</sub>/Cl, *vide supra*).<sup>25</sup>

Even though the crystal structures of ADPO·Cr(CO)<sub>5</sub> and ADPO·W(CO)<sub>5</sub> have not been reported there is no doubt (because of the characteristic NMR data discussed above) about the 8-P-4 geometric arrangements in the complexes which appear to arise from the 8-P-3 ADPO electromorph rather than the planar 10-P-3 ADPO.<sup>59</sup>

#### B. Complexes with the Transition Group 7 Metal, Mn

ADPO forms a 1:1 adduct with the MnCp(CO)<sub>2</sub> fragment (eq 24).<sup>64</sup> The structure of ADPO·MnCp-

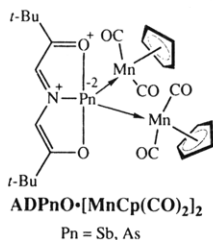


(CO)<sub>2</sub> has been confirmed by X-ray crystallographic studies and shows an 8-P-4 coordination mode with a fold angle of 117° between the two five-membered rings



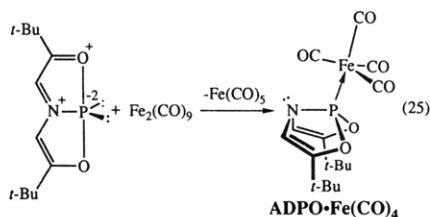
of the ADPO ligand. In solution, multinuclear magnetic resonance spectra also support the 8-P-4 structure. The two ring protons in the ligand backbone shift upfield in the ADPO·MnCp(CO)<sub>2</sub> adduct to 5.74 ppm (*cf.* δ 7.5 for ADPO). Also, the phosphorus coupling to these protons increases from 9.6 Hz for uncomplexed ADPO to 24.3 Hz in the manganese complex. The C<sub>3(7)</sub> centers resonate at δ 155.2, 14.7 ppm upfield from their chemical shift in uncomplexed ADPO. The <sup>31</sup>P NMR chemical shift of δ 256 does not readily correlate with any specific structural feature of the ADPO·MnCp(CO)<sub>2</sub> complex, a problem common among ADPO metal adducts.

The same 1:1 ADPO·MnCp(CO)<sub>2</sub> adduct is formed even when 2 equiv of MnCp(CO)<sub>2</sub>·thf are used in the reaction. This result stands in contrast to the formation of 10-Sb-5 antimony-bridged ADSbO·[MnCp(CO)<sub>2</sub>]<sub>2</sub> and 10-As-5 arsenic-bridged ADAso·[MnCp(CO)<sub>2</sub>]<sub>2</sub>.<sup>64</sup> This marked difference between 10-P-3 ADPO on the one hand and 10-Sb-3 ADSbO or 10-As-3 ADAso on the other is tied to the energy balance on the surface which connects the 10-Pn-3 and 8-Pn-3 ADPnO electromorphs. The energy difference between the 10-P-3 and 8-P-3 electromorph of ADPO was calculated to be 13.9 kcal mol<sup>-1</sup> (in favor of the planar 10-P-3 structure).<sup>14</sup> The difference between the 10-As-3 and 8-As-3 electromorphs of ADAso was calculated to be 23.0 kcal mol<sup>-1</sup> and the difference in the antimony structures is expected to be even greater.<sup>14</sup> The small energy difference in the 10-P-3 and 8-P-3 electromorphs of ADPO is easily overcome by the strong bond energies associated with the formation metal-phosphorus complexes and this is believed lead to the preference for an 8-P-4 arrangement for most metal complexes of ADPO compared to the 10-Pn-4 or 10-Pn-5 arrangements that are preferred for arsenic- and antimony-derived systems.



### C. Complexes with the Transition Group 8 Metals, Fe and Ru

ADPO reacts with Fe<sub>2</sub>(CO)<sub>9</sub> at room temperature in pentane over several hours. The iron carbonyl slowly dissolves to give ADPO·Fe(CO)<sub>4</sub> in quantitative yield (eq 25).<sup>63</sup> This same adduct has also been formed by the reaction of ADPO·Cl<sub>2</sub> with Na<sub>2</sub>[Fe(CO)<sub>4</sub>]<sub>2</sub>.<sup>63</sup>



The IR spectrum of ADPO·Fe(CO)<sub>4</sub> shows the typical ν<sub>CO</sub> for an axially substituted LFe(CO)<sub>4</sub>.<sup>65</sup> However, the bands are at a higher frequency compared to other

LFe(CO)<sub>4</sub> (L = alkyl<sub>3</sub>P,<sup>66</sup> Ph<sub>3</sub>P,<sup>66</sup> (Me<sub>2</sub>N)<sub>3</sub>P<sup>67</sup>) and even higher than for (MeO)<sub>3</sub>PFe(CO)<sub>4</sub>,<sup>66</sup> which suggests that folded ADPO is a good π-acceptor. The <sup>1</sup>H NMR shift of the ring protons exhibit the expected upfield shift (δ 7.50 → 5.89) with the corresponding increase in <sup>3</sup>J<sub>PH</sub> (9.6 Hz → 26.4 Hz) when going from free ADPO to a complexed, folded 8-P-4 ADPO structure. The C<sub>3(7)</sub> resonances are shifted upfield by 13.5 ppm similar to other metal complexes.

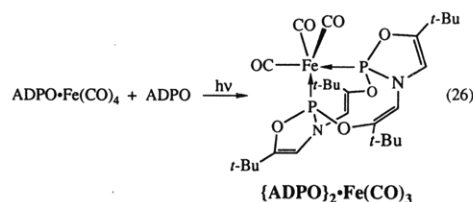
Single-crystal X-ray diffraction analysis of the complex confirmed the structure of ADPO·Fe(CO)<sub>4</sub> and found a ring fold of 116.5°. The ADPO ligand is roughly tetrahedral, with the iron being approximately *tbp* and the phosphorus occupying one axial site. The Fe–P bond distance is about 8 pm shorter than the corresponding distances in most other phosphorus–iron–(carbonyl) complexes (L = (Me<sub>2</sub>N)<sub>3</sub>P,<sup>68</sup> Ph<sub>3</sub>P,<sup>69</sup> Ph<sub>2</sub>HP<sup>70</sup>). However, the Fe–P distance is approximately the same as those found in a few phosphorus–iron–(carbonyl) compounds in which the four-coordinate phosphorus center bears substituents that would favor

an edge-inversion process (*e.g.* [(Me)NCH<sub>2</sub>CH<sub>2</sub>N–(Me)P(F)]Fe(CO)<sub>4</sub><sup>71</sup> and the adduct of the saturated analog 2 of ADPO and Cp(C<sub>6</sub>H<sub>5</sub>)(CO)Fe<sup>72</sup>). The short Fe–P bond distances in these latter adducts are most certainly due to the π-acceptor properties of the coordinated phosphorus centers as a square-planar edge inversion transition state is approached.<sup>14</sup> The square-planar edge-inversion transition-state structure **19** was investigated by density functional theory and found to be only 0.68 kcal mol<sup>-1</sup> above the ground-state structure.<sup>63</sup>



Structure **19** represents a bonding mode in ADPO-metal complexes that corresponds to a double σ and ππ–dπ interaction. Although such a ground-state structure has not yet been observed, the very low energy of the transition-state structure **19** suggests that such a representative of planar four-coordinate phosphorus might be possible.

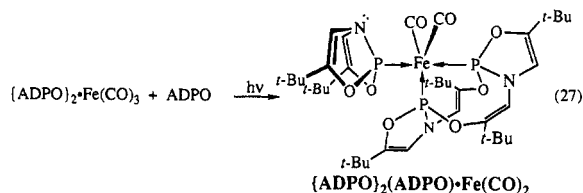
Another equivalent of ADPO will react with ADPO·Fe(CO)<sub>4</sub> in cyclohexane under UV irradiation to give the disubstituted species, {ADPO}<sub>2</sub>·Fe(CO)<sub>3</sub> (eq 26).<sup>28,63</sup>



The complex, {ADPO}<sub>2</sub>·Fe(CO)<sub>3</sub> is not simply the complex of two isolated ADPO units on a single Fe(CO)<sub>3</sub> center. The IR spectrum of {ADPO}<sub>2</sub>·Fe(CO)<sub>3</sub> suggests a *cis* geometry about the iron center. Two sets of resonances for the *tert*-butyls, ring carbons, and ring protons in the NMR spectra indicate the basic

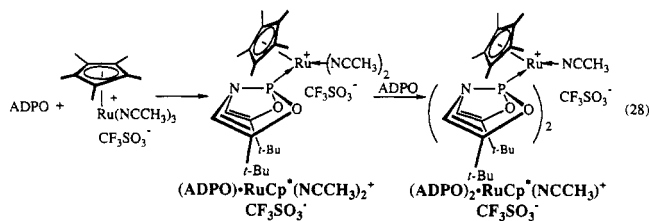
bicyclic ring structure of the ADPO fragments was disrupted. The  $^{31}\text{P}$  NMR spectrum shows a single phosphorus resonance (because of pseudorotation at iron) at  $\delta$  132 ppm. On the NMR time scale one resonance is observed for the three iron carbonyl ( $\text{C}\equiv\text{O}$ ) carbon atoms, which is split into a triplet due to the coupling from the two averaged phosphorus atoms. The NMR data support an 8-P-4 arrangement in which the symmetry of the ADPO unit was destroyed. The X-ray structure determination of  $\{\text{ADPO}\}_2\cdot\text{Fe}(\text{CO})_3$  confirms the axial/equatorial arrangement of the two phosphorus atoms. The structure also reveals that the two ADPO units have dimerized ( $\{\text{ADPO}\}_2$ )<sup>28</sup> via P–O bond cleavage to transform two of the five-membered rings into a 10-membered ring. Although Wolf and co-workers have reported the dimerization of their saturated analog 13 of ADPO compounds,<sup>21,24</sup>  $\{\text{ADPO}\}_2\cdot\text{Fe}(\text{CO})_3$  provides the first example of ADPO dimerization (although complexed). Attempts to recover the isolated ADPO dimer ( $\{\text{ADPO}\}_2$ ) by liberation from  $\{\text{ADPO}\}_2\cdot\text{Fe}(\text{CO})_3$  under pressure of excess carbon monoxide afforded only monomeric 10-P-3 ADPO. This suggests reversion of the  $\{\text{ADPO}\}_2$  to the monomer is quite facile (*vide infra*).

Another equivalent of ADPO can be added to  $\{\text{ADPO}\}_2\cdot\text{Fe}(\text{CO})_3$  under UV irradiation (eq 27).<sup>63</sup> The



product formed has two  $^{31}\text{P}$  resonances, one is a doublet at  $\delta$  174, while the other is a triplet at  $\delta$  240 ( $J_{\text{PP}} = 21.7$  Hz). These resonances are similar to  $\{\text{ADPO}\}_2\cdot\text{Fe}(\text{CO})_3$  and  $\text{ADPO}\cdot\text{Fe}(\text{CO})_4$ , respectively, and imply that the third ADPO complexes as a single unit and does not insert into the dimerized ADPO units to form a trimer. Additional  $^{13}\text{C}$  and  $^1\text{H}$  NMR data support the monomer/dimer character in the  $\{\text{ADPO}\}_2(\text{ADPO})\cdot\text{Fe}(\text{CO})_2$  complex. Further incorporation of ADPO into  $\{\text{ADPO}\}_2\cdot\text{Fe}(\text{CO})_2$  was not observed.

The electrophilic ruthenium center in  $[\text{Cp}^*(\text{CH}_3\text{CN})_3\text{Ru}]^+[\text{O}_3\text{SCF}_3]^-$  will also coordinate ADPO with the liberation of acetonitrile (eq 28).<sup>62</sup> One or two equivalents of ADPO can be added depending on the stoichiometry employed and in each case the mono- or disubstituted ADPO complexes can be isolated.



The  $^1\text{H}$  and  $^{13}\text{C}$  chemical shifts of both of these complexes are indicative of a reduced ligand backbone and thus the folded 8-P-4 arrangement of the ADPO ligand. The 1:1 adduct shows the expected upfield shift for ring protons and the  $\text{C}_{3(7)}$  carbons ( $\delta$  5.79,  $^3J_{\text{PH}} = 24.1$  Hz and  $\delta$  155.6, respectively). The 2:1 adduct

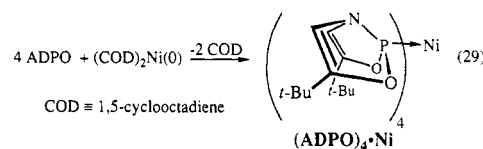
exhibits similar ring proton and  $\text{C}_{3(7)}$  chemical shifts ( $\delta$  5.82 and  $\delta$  155.9), however the spectrum was complicated by virtual couplings to both phosphorus atoms. Nonetheless it is clear that the two ADPO units are not dimerized in this 2:1 ruthenium adduct. It was not possible to displace the last acetonitrile with an excess of ADPO.

The failure of the  $(\text{ADPO})_2\cdot\text{RuCp}^*(\text{NCCH}_3)^+$  to form an ADPO dimer fragment is believed to be due to the greater distance between phosphorus in the tetrahedral ruthenium environment compared to the *tbp* five-coordinate iron environment for a  $(\text{ADPO})_2\cdot\text{Fe}(\text{CO})_3$  structure.<sup>69</sup> For dimerization between ADPO subunits to occur, the phosphorus atoms seem to need to approach one another within about 325 pm (*vide infra*) in the idealized geometry of a precursor made up of only monomeric units. For structures containing an  $(\text{R}_3\text{P})_2\text{RuCp}^*(\text{L})$  functionality the distance between nonbonded phosphorus atoms ranges between 328 and 345 pm with an average of 333 pm.<sup>79–76</sup> Thus it seems likely that the ADPO subunits in  $(\text{ADPO})_2\cdot\text{RuCp}^*(\text{NCCH}_3)^+$  are too far apart to dimerize.

As with many other metal centers, the heavier analogs of ADPO, ADAso, and ADSbo, show different structures for their ruthenium complexes. A 3:1 ADSbo adduct of the  $\text{RuCp}^{*+}$  center has been reported and found to contain three  $\psi$ -*tbp* 10-Sb-4 centers so that the planarity of the ADSbo subunit is maintained.<sup>62</sup>

#### D. Complexes with the Transition Group 10 Metals, Ni, Pd, and Pt

Using bis(cyclooctadiene)nickel as a Ni(0) source  $(\text{ADPO})_4\cdot\text{Ni}$  can be prepared (eq 29).<sup>59</sup> As with a



majority of the other ADPO metal complexes, the ligated ADPO fragment adopts the folded 8-P-4 configuration as evidenced by the NMR chemical shifts of the ring protons ( $\delta$  5.4) and  $\text{C}_{3(7)}$  carbons ( $\delta$  153.5). The coupling between phosphorus and the ring protons is again complicated by virtual coupling to all of the phosphorus centers. Since single resonances are found for the *tert*-butyls and ring carbons, a complex composed of only monomeric ADPO subunits is expected. This homoleptic  $(\text{ADPO})_4\cdot\text{Ni}(0)$  arrangement was confirmed by X-ray crystallography.

The four ADPO molecules are arranged tetrahedrally around the nickel center and are too far apart to dimerize. The average P–P distance in  $(\text{ADPO})_4\cdot\text{Ni}$  is 342 pm with the closest distance between two phosphorus atoms at 329 pm. This value exceeds the 325-pm distance that seems to be the maximum at which ADPO dimerization can occur (*vide infra*). The structure of homoleptic  $(\text{ADPO})_4\cdot\text{Ni}$  is shown in Figure 7. The ring fold angles in the ADPO subunits are 114.1°, 116.9°, 117.5°, and 118.8°.

In contrast to the  $(\text{ADPO})_4\cdot\text{Ni}$  complex which contains four discrete ADPO units, tetrakis(acetonitrile)-palladium(II) tetrafluoroborate reacts with four equiva-

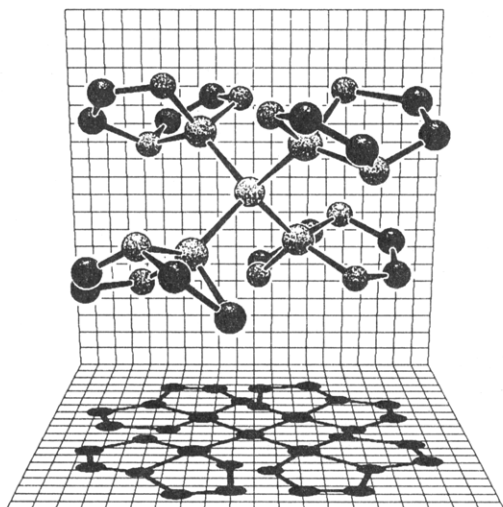


Figure 7. KANVAS<sup>42</sup> drawing of (ADPO)<sub>4</sub>·Ni. (*tert*-Butyls and hydrogens have been omitted for clarity.)

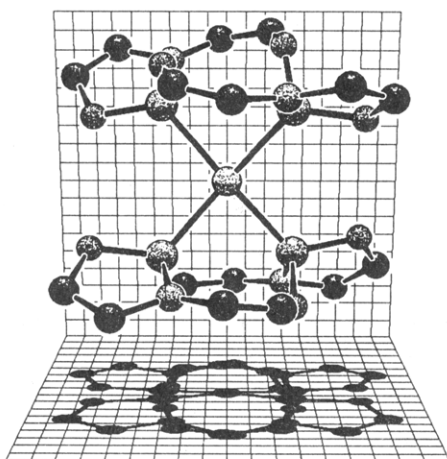
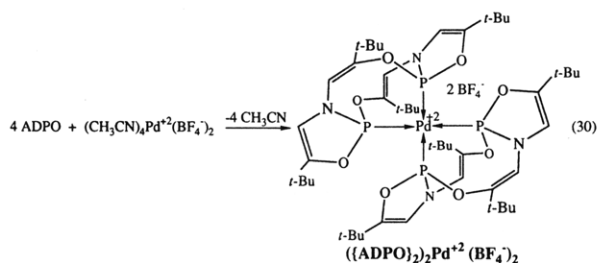


Figure 8. KANVAS<sup>42</sup> drawing of ({ADPO}<sub>2</sub>)<sub>2</sub>Pd<sup>2+</sup>. (*tert*-Butyl and hydrogens have been omitted for clarity.)

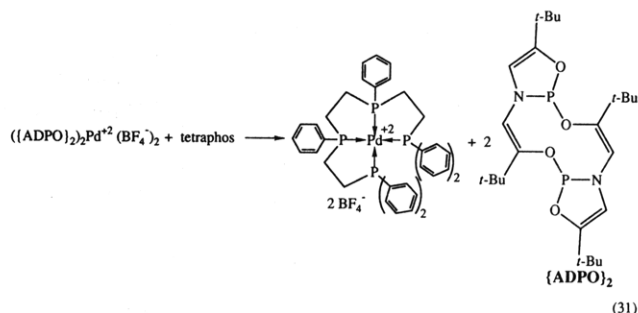
lents of ADPO to give [(ADPO)<sub>2</sub>]<sub>2</sub>·Pd<sup>2+</sup>[BF<sub>4</sub>]<sup>-</sup> in which two sets of ADPO subunits dimerize (eq 30).



The dimerization of these two sets of ADPO units is signaled by the <sup>1</sup>H NMR spectrum which exhibits two sets of *tert*-butyl and vinyl proton resonances for the substituents on the five- and 10-membered rings. The apparently identical couplings of the four phosphorus atoms to the vinyl protons cause these protons to appear as quintets, a problem similar to the virtual couplings observed in (ADPO)<sub>4</sub>·Ni, {ADPO}<sub>2</sub>·Fe(CO)<sub>3</sub> and (ADPO)<sub>2</sub>·RuCp<sup>+</sup>(NCCH<sub>3</sub>)<sup>+</sup> (*vide supra*). Single-crystal X-ray diffraction studies show the geometry of the palladium to be square planar (Figure 8). The close proximity of the phosphorus atoms arranged in the square plane about the palladium atom is responsible for dimerization of the ADPO units. In an idealized

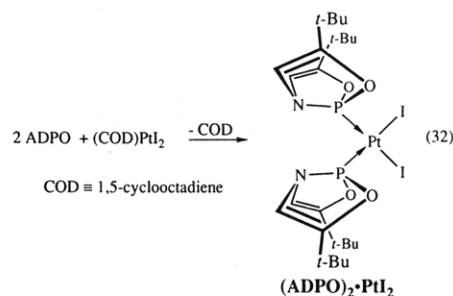
square-planar arrangement of four phosphorus centers about a palladium (assuming the average P–Pd distance in [(ADPO)<sub>2</sub>]<sub>2</sub>·Pd<sup>2+</sup>[BF<sub>4</sub>]<sup>-</sup>), adjacent phosphorus atoms approach within 324 pm. This is actually the largest distance at which dimerization of ADPO subunits has been observed.

Unlike {ADPO}<sub>2</sub>·Fe(CO)<sub>3</sub>, liberation and detection of the intact dimer ADPO unit, {ADPO}<sub>2</sub>, from [(ADPO)<sub>2</sub>]<sub>2</sub>·Pd<sup>2+</sup> was possible. Reaction of [(ADPO)<sub>2</sub>]<sub>2</sub>·Pd<sup>2+</sup>[BF<sub>4</sub>]<sup>-</sup> with tetraphos([(C<sub>6</sub>H<sub>5</sub>)<sub>2</sub>-PCH<sub>2</sub>CH<sub>2</sub>P(C<sub>6</sub>H<sub>5</sub>)CH<sub>2</sub>]<sub>2</sub>) provided <sup>31</sup>P and <sup>1</sup>H NMR evidence for the presence of free {ADPO}<sub>2</sub> (eq 31).<sup>59</sup>



The liberated {ADPO}<sub>2</sub> showed a <sup>31</sup>P chemical shift of δ 133.9 and <sup>1</sup>H chemical shifts at δ 1.19 (s, *tert*-Bu), 1.130 (s, *tert*-Bu), 5.60 (pseudo t, 5.08 Hz), and 5.71 (pseudo t, 2.36 Hz). This new <sup>31</sup>P resonance is similar to the dimer of saturated ADPO analogs 13 studied by Wolf and co-workers (Table 4).<sup>21,24</sup> However, unlike the saturated dimers 14, {ADPO}<sub>2</sub> readily converts to 10-P-3 ADPO at room temperature which precluded isolation or further characterization.

The first metal complex synthesized from ADPO was a bisADPO complex of *cis*-PtI<sub>2</sub>. This complex was prepared by the reaction of 2 equiv of ADPO with (1,5-cyclooctadiene)platinum diiodide (eq 32).<sup>25,60</sup> The 2:1 stoichiometry of the yellow crystalline compound was determined by elemental analysis, NMR spectra, and X-ray crystallography.



The C<sub>3(7)</sub> and ring proton resonances show very substantial upfield chemical shifts in (ADPO)<sub>2</sub>·PtI<sub>2</sub> relative to 10-P-3 ADPO (Δδ = 23.9 and 1.5 ppm, respectively). The <sup>3</sup>J<sub>PH</sub> coupling constant in the ADPO unit increases from 9.6 to 29.0 Hz on complexation while <sup>1</sup>J<sub>PN</sub> decreases from 80.0 to 44.8 Hz. The <sup>1</sup>J<sub>PN</sub> coupling constant in ADPO-derived compounds has been shown to track the phosphorus coordination number and in this case indicates the expected four-coordinate geometry.<sup>25</sup> As noted previously these chemical shift and coupling constant changes have all been shown to be indicative of oxidation of the phosphorus center and folding of the previously planar 10-P-3 ADPO ring

system.<sup>25,60</sup> In addition to these NMR data, the <sup>15</sup>N resonance in (ADPO)<sub>2</sub>PtI<sub>2</sub> shows a very large upfield shift ( $\Delta\delta = 149.7$  ppm) relative to 10-P-3 ADPO. This nitrogen resonance is a particularly sensitive measure of the presence or absence of a lone pair of electrons on nitrogen thereby indicating internal redox changes in the phosphorus/organic ligand system.

In planar 10-P-3 ADPO the lone pairs of electrons can be formulated as either two sets of sp<sup>2</sup> hybrids or as an sp + p set (*vide supra* structure 7a). Upon complexation to the platinum center, the ADPO molecule reorganizes structurally and electronically. Structurally, the ADPO fragment goes from planar to folded. In converting to a folded, 8-P-3 center (actually an 8-P-4 center in the complex), electron density is returned to the nitrogen (as a lone pair of electrons) and a pyramidal geometry is adopted. This places the remaining lone pair of electrons at phosphorus in a more directional sp<sup>3</sup> orbital for better overlap with the platinum and provides a sterically more accessible phosphorus center.

The structure of (ADPO)<sub>2</sub>PtI<sub>2</sub> was proven by single-crystal X-ray diffraction.<sup>60</sup> The ADPO molecule is folded with an angle of 119° between the two five-membered rings. The N–P bond distance in the complexed ligand is only 2 pm longer than in the free 10-P-3 ADPO. The  $\pi$ -bonds in the ligand ring backbone are fixed as evidenced by the increased C–O and C–N bonds and shortened C=C bonds (Table 1). These findings are in accord with expectations based on the required electronic changes on going from a planar to a folded structure.

In contrast to the folded 8-P-4 arrangement found in ADPO–platinum complexes, the antimony analog, ADSbO, forms the planar 10-Sb-4 arrangements with platinum centers.<sup>60,77</sup>

It is worth noting that a folded 8-P-3 ADPO molecule could not be liberated from (ADPO)<sub>2</sub>PtI<sub>2</sub> or any of the previously described metal complexes that contain the folded 8-P-4 ADPO moiety. When it was possible to release an ADPO unit, the freed ADPO molecule exhibited the planar 10-P-3 arrangement. Transformation to the planar 10-P-3 geometry may be concurrent with displacement from the metal center or the conversion of folded 8-P-3 ADPO to planar 10-P-3 ADPO may proceed with a very low activation energy as expected on the basis of theoretical models.<sup>14,25,63</sup>

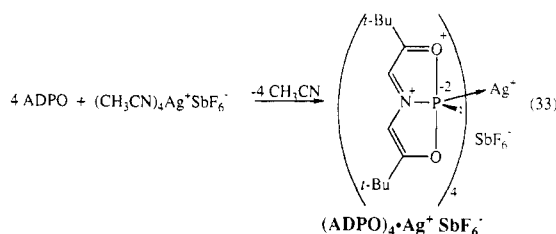
### E. Complexes with the Transition Group 11 Metal, Ag

The silver ADPO complexes are among the most recent adducts to be reported and represent a noteworthy milestone in the chemistry of the low-coordinate hypervalent ADPO compounds. It is in these silver complexes that both the  $\psi$ -tbp 10-P-4 and bridging 10-P-5 arrangements are seen for the first time. These silver adducts support the validity of the resonance representation 7a for the ground state of ADPO and lend support for the calculated energy difference between the 8-P-3 and 10-P-3 electromorphs of ADPO.

The energy difference between planar 10-P-3 ADPO and folded 8-P-3 ADPO is calculated to be 13.9 kcal mol<sup>-1</sup> in favor of the planar structure. If 10-P-4 or 10-P-5 arrangements are to be observed in metal complexes this delicate energy balance cannot be disturbed. The

metal complexes of ADPO described above have high enough P → M bond strengths to disrupt the 8-P-3 *vs* 10-P-3 ADPO balance. This high phosphorus–metal bond strength encourages folding the coordinated ADPO molecule to provide a sterically more accessible phosphorus center and a more basic sp<sup>3</sup> phosphorus lone pair of electrons to participate in the strong metal phosphorus bonds. Once this effect was understood the simple strategy of using a weakly coordinating metal center produced the examples of the previously unknown 10-P-4 and 10-P-5 metal complexes. Silver(I) centers are known to have low P → Ag bond strengths with dissociation energies of less than 11 kcal/mol.<sup>78</sup>

The first example of a transition-metal complex containing a  $\psi$ -tbp 10-P-4 phosphorus center was obtained by the reaction of [Ag(NCCH<sub>3</sub>)<sub>4</sub>]<sup>+</sup>SbF<sub>6</sub><sup>-</sup> with 4 equiv of ADPO (eq 33).<sup>79</sup>



The <sup>1</sup>H NMR shift of the ring protons is consistent with the planar, oxidized ligand ring system. There was an increase in <sup>3</sup>J<sub>PH</sub> (9.6 → 14.3 Hz), which corresponds to only about 30% of the increase typically found in 8-P-4 complexes of ADPO (*vide supra*). Some increase in <sup>3</sup>J<sub>PH</sub> is expected with an increase in coordination number for phosphorus. The <sup>15</sup>N NMR chemical shift ( $\delta - 124.5$ , <sup>1</sup>J<sub>PN</sub> = 64.4 Hz) is very similar to uncomplexed, planar 10-P-3 ADPO and indicates there has been no change in the relative oxidation states phosphorus and the organic ligand backbone of ADPO as usually occurs in 8-P-4 complexes. This slight reduction in P–N coupling follows previous trends compatible with an increase in phosphorus coordination number but the reduction is only about 44% of what would be expected.<sup>25</sup> It was found that the ADPO ligands in [(ADPO)<sub>4</sub>Ag]<sup>+</sup>SbF<sub>6</sub><sup>-</sup> were very labile, and average chemical shifts and coupling constants were observed when excess ADPO ligand was added to a CD<sub>2</sub>Cl<sub>2</sub> solution of the complex. This lability explains the absence of Ag–P coupling even at –95 °C and is consistent with a weak P → Ag interaction. The rapid dissociation of ADPO ligands from the silver center in solution precludes a specific characterization of NMR chemical shifts since only averaged values are seen.

The X-ray crystal structure of [(ADPO)<sub>4</sub>Ag]<sup>+</sup> is shown in Figure 9. It is of interest to note that the silver atom is in a square-planar geometry, this is unusual for an 18e silver cation.<sup>80,81</sup> The homoleptic [(ADPO)<sub>4</sub>Ag]<sup>+</sup> is isoelectronic with (ADPO)<sub>4</sub>Ni, but the geometries of the metals and ADPO fragments are very different. In [(ADPO)<sub>4</sub>Ag]<sup>+</sup> the complexed ADPO ligand is essentially planar and the structure is very similar to uncomplexed 10-P-3 ADPO (fold angle = 175°). The remaining, uncomplexed lone pair of electrons at the phosphorus atom is stereochemically active as evidenced by the Ag–P–N bond angle of 113.1°. The P–Ag bond distance is slightly shorter (261.2 pm) than bond distances in Ag(PPh<sub>3</sub>)<sub>4</sub><sup>+</sup> (typical P–Ag bond

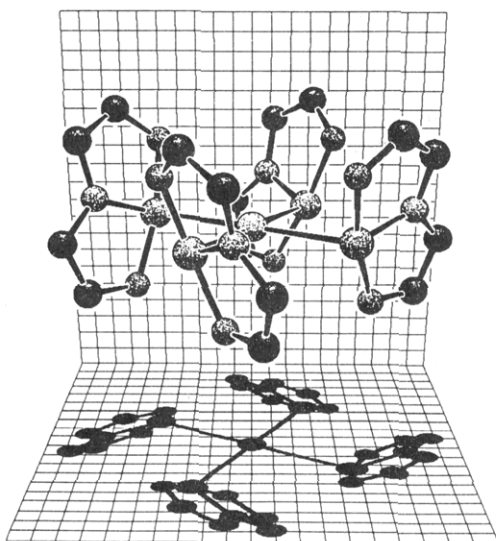


**Figure 9.** KANVAS<sup>34</sup> drawing of [(ADPO)<sub>4</sub>Ag]<sup>+</sup>. (Hydrogens and *tert*-butyls have been omitted for clarity.)

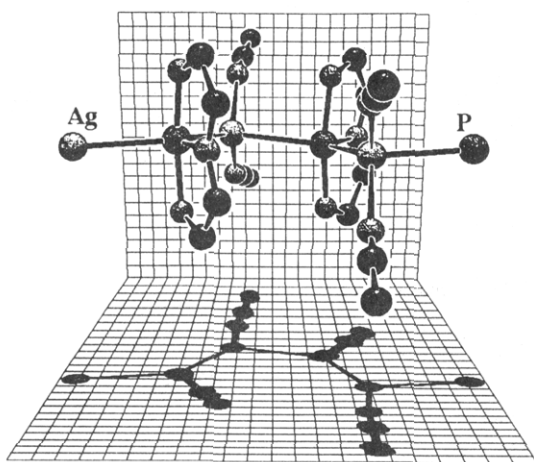
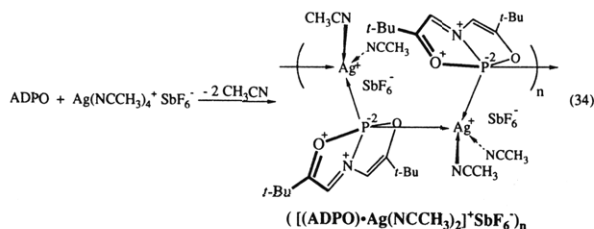


**Figure 10.** KANVAS<sup>42</sup> drawing of [(ADPO)·Ag(NCCH<sub>3</sub>)<sub>2</sub>]<sup>+</sup>·SbF<sub>6</sub><sup>-</sup><sub>n</sub>. (Hydrogens and *tert*-butyls have been omitted for clarity.)

distances range from 261.5 to 274.6 pm).<sup>79</sup> The solid-state geometry of [(ADPO)<sub>4</sub>Ag]<sup>+</sup> clearly contains the 10-P-4 ligation arrangement for the ADPO ligands.

If the stoichiometry of the ADPO + Ag(NCCH<sub>3</sub>)<sub>4</sub><sup>+</sup> reaction is changed to 1:1, a polymeric structure can be prepared (eq 34).<sup>82</sup> Unlike the [(ADPO)<sub>4</sub>Ag]<sup>+</sup> complex, the phosphorus in ADPO acts as four-electron donor to give a bridged 10-P-5 ADPO species.



Even though the solid-state structure (Figure 10) is polymeric this 1:1 complex is very soluble in CH<sub>2</sub>Cl<sub>2</sub>, but slowly decomposes at room temperature. The precise structure of the adduct in solution is unknown and retention of the extended polymeric structure seems unlikely. Lower molecular weight cyclic oligomers or short linear chains terminated by solvent molecules

are possible. Again the ADPO is loosely coordinated to the silver center as evidenced by the displacement of ADPO by donor solvents such as thf and acetonitrile. The <sup>1</sup>H and <sup>13</sup>C NMR chemical shifts (CD<sub>2</sub>Cl<sub>2</sub>) for the complex are similar to those of the uncomplexed ADPO. The <sup>3</sup>J<sub>PH</sub> coupling constant of 18.1 Hz for the complex's rings protons is larger than for free ADPO as expected. This coupling follows the same trend as the 4:1 adduct, [(ADPO)<sub>4</sub>Ag]<sup>+</sup>, but probably also reflects a dynamically averaged value. When the solution is cooled, a slight downfield shift of the ring protons and upfield shift of the phosphorus resonance is seen, (δ 7.94 (20 °C) → 8.08 (−90 °C), δ 152 (20 °C) → 139 (−90 °C) respectively). The low-temperature shift of the phosphorus resonance is identical to the solid-state <sup>31</sup>P shift and suggests that at low temperatures solutions of this 1:1 adduct contain species structurally similar to the extended polymer found in the solid state.

The structural features of [(ADPO)<sub>2</sub>Ag(NCCH<sub>3</sub>)<sub>2</sub>]<sup>+</sup>SbF<sub>6</sub><sup>-</sup><sub>n</sub> were determined by X-ray diffraction studies. There are several features to note in this structure. The complex is actually a polymeric, zigzag thread of alternating silver and phosphorus atoms. The phosphorus performs a bridging four-electron donor role as a *tbp* 10-P-5 center and the silver centers are tetrahedral, unlike the previous structure, [(ADPO)<sub>4</sub>Ag]<sup>+</sup>SbF<sub>6</sub><sup>-</sup>. The *tbp* structure at phosphorus places two silver atoms and nitrogen in equatorial positions with the axial positions occupied by the oxygens. The Ag–P–Ag bond angle is 131.5(2)°, which is about 12° larger than the idealized *tbp* geometry, but follows the trend set by the heavier 10-P<sub>n</sub>-5 congeners (As and Sb).<sup>64</sup> The ADPO ring system is essentially planar with a 179° angle between the two five-membered rings.

## X. Conclusions

Low-coordinate hypervalent phosphorus compounds are known both as intermediates and as ground-state structures. The ADPO compounds are stable ground-state structures representing the 10-electron, three-coordinate (10-P-3) bonding arrangement (7a). The 10-P-3 ground state structures in the ADPO series are closely tied to the octet-rule-obeying 8-P-3 structures which are also minima on the potential energy surface. These folded 8-P-3 structures are only about 14 kcal mol<sup>-1</sup> above the planar 10-P-3 ADPO ground-state structure. The contribution of the folded 8-P-3 arrangement to the chemistry of ADPO is evident when the incoming reagents form bonds to the phosphorus center with bond energies in excess of the 14 kcal mol<sup>-1</sup>.

The electromorphism possible in the ADPO system between the 8-P-3 and 10-P-3 arrangements led to the discovery of a new edge-inversion process for three-coordinate pnictogen compounds. The ground state 10-P-3 ADPO structure is actually a model of the transition state for this inversion process. This edge inversion process has now experimentally been verified at phosphorus and bismuth centers in the pnictogen family and the process has been extended to tetrahedral four-coordinate centers like silicon and germanium. An inversion process at carbon which would involve a square-planar transition state has long been a goal in organic chemistry, and the understanding which has developed from known edge-inversion processes in the

main group IV and V families can now contribute to this quest.

Multinuclear magnetic resonance spectra are especially helpful in characterizing the geometries and electronic arrangements in ADPO-derived compounds. Data from both coupling constants and chemical shifts have been correlated with various electronic and geometric arrangements. The  $^1\text{H}$  chemical shifts of the ring protons with their 3-bond coupling constants to phosphorus along with  $^{15}\text{N}$  chemical shifts have proven the most reliable indicators. The utility of  $^{31}\text{P}$  NMR for determining phosphorus coordination number and geometry is less reliable for transition metal derived complexes where the chemical shift is strongly influenced by effects of the metal center.

If a normal 8-P-3 (phosphine) arrangement is regarded as P(III), the phosphorus center in 10-P-3 structures should be regarded as P(I) by virtue of the presence of an additional lone pair of electrons over the 8-P-3 structure. Oxidative addition of reagents like quinones, halogens, hydrogen, or alcohols to the phosphorus center of ADPO transforms the P(I) center into a P(V) center. The 10-P-5 centers that result from oxidative addition to the phosphorus center of ADPO have bypassed the P(III) oxidation state as a result of participation of the organic ligand backbone of ADPO. One lone pair of electrons at phosphorus is required for an oxidative addition at this center and the second lone pair of electrons which was originally present in the 10-P-3 arrangement is transferred to the organic ligand backbone. This behavior is contrary to that which is observed with heavier pnictogen centers, arsenic and antimony, from which oxidation state III 12-Pn-5 arrangements are formed by oxidative additions to the pnictogen centers of ADAsO or ADSbO.

ADPO is an excellent ligand for transition metal centers. The ADPO group can be ligated to a metal center in a number of different ways. Bridging 10-P-5 and  $\psi$ -tbp 10-P-4 arrangements are rare but have been observed at silver centers. With most transition metal centers the P  $\rightarrow$  metal bond strength is sufficiently high to disturb the electromorphic balance between the 10-P-3 and 8-P-3 structures. As a result of these strong metal-phosphorus interactions 8-P-4 tetrahedral phosphorus geometries are found for most metal adducts. Theoretical models predict that compounds that possess a  $p\pi-d\pi + \sigma$  double interaction between phosphorus and a metal center are possible and will result in formation of a square-planar geometry at the phosphorus center. Searches for this square-planar arrangement are ongoing. The behavior ADPO toward metal complexation is again contrasted by the heavier congeners, ADAsO and ADSbO, from which 10-Pn-4 and 10-Pn-5 arrangements are common and 8-Pn-4 arrangements are unknown.

## XI. Abbreviations

DZP	double $\zeta$ polarized (basis set)
HFB	hexafluoro-2-butyne
HFBA	hexafluorobiacytyl
HFPO	hexafluoropropylene oxide
HOTf	triflic acid, trifluoromethanesulfonic acid, $\text{CF}_3\text{-SO}_3\text{H}$
IR	infrared spectroscopy
MeOH	methanol

MP-2	Møller-Plesset (second-order correlation correction)
NMR	nuclear magnetic resonance
ROP	ring-opening polymerization
SCF	self-consistent field (molecular orbital calculation)
TASF	tris(dimethylamido)sulfonium difluorotrimethylsilicate
tbp	trigonal bipyramid
thf	tetrahydrofuran
$\psi$ -tbp	pseudo-trigonal bipyramid

## XII. References

- Arduengo, A. J., III; Dias, H. V. R. *Main Group Chem. News* 1994, 2, 16.
- The N-X-L nomenclature system has been previously described (Perkins, C. W.; Martin, J. C.; Arduengo, A. J., III; Lau, W.; Algeria, A.; Kochi, J. K. *J. Am. Chem. Soc.* 1980, 102, 7753). N valence electrons about a central atom X, with L ligands.
- Because of the number of structurally diverse compounds discussed in this review we have used acronyms derived from the name of the central ring system, 5-aza-2,8-dioxo-1-phosphabicyclo[3.3.0]octa-2,4,6-triene (ADPO). The central element in this ring system can be substituted with other elements in the "pnictogen" family (i.e. ADPO, Pn = As, ADAsO). The terms "pnictogen" and "pnictide" have been used to refer to the main group V (group 15) elements (N, P, As, Sb, Bi). These terms are derived from the Greek word pniktos (suffocate—the origin of the prefix "pnicto"). See: Brown, R. W. *Composition of Scientific Words*; George W. King Printing Co.: Baltimore, MD, 1954; p 620. The terms "pnigogen" and "pnicogen" have also been used to identify this family of elements (Suchow, L. *Inorg. Chem.* 1978, 17, 2041). The latter two terms are somewhat inappropriate since *pnigo* (the source of pnigogen) means "choke" rather than "suffocate" and "pnicogen" does not reflect the proper etymology (the "t" should not be omitted). For the spoken words, the terms "pnictogen" and "pnictide" are clearly and easily enunciated. Thus we prefer the terms derived from "pnicto" (pnictogen and pnictide). The acronyms are identified with the drawings in the text. Prefixes are added to indicate substituents in the 3 and 7 positions (e.g., di-*t*-Bu-ADPO, dicumyl/ADPO, etc.). However, most of the chemistry of the ADPO molecules has been studied with the 3,7-di-*tert*-butyl derivative and for convenience the ADPO acronym is used to mean di-*t*-Bu-ADPO. Products derived from the parent ADPO systems are identified by adding a suffix to the acronym which identifies the elements are groups that are chemically incorporated (e.g., ADPO-Cl<sub>2</sub> for the adduct of ADPO and two atoms of chlorine). The "-" used to append the suffix indicates composition but not the nature of the bonds formed.
- Culley, S. A.; Arduengo, A. J., III. *Abstracts of Papers*, 186th National Meeting of the American Chemical Society, Washington, DC; American Chemical Society: Washington, DC, 1983; ORGN 110.
- Lochs Schmidt, S.; Schmidpeter, A. Z. *Naturforsch.* 1985, 40b, 765.
- As we have previously stressed it is important to realize that the atomic charges assigned in the 10-P-3 ADPO structure are formal, and not actual charges; see ref 25.
- Sanchez, M.; Mazières, M.-R.; Lamandé, L.; Wolf, R. Phosphonium Ions. In *Multiple Bonds and Low Coordination in Phosphorus Chemistry*; Regitz, M., Scherer, O. J., Eds.; Verlag Chemie: New York, 1990; p 129.
- Mathey, F. Phosphorus Compounds with Coordination 1. In *Multiple Bonds and Low Coordination in Phosphorus Chemistry*; Regitz, M., Scherer, O. J., Eds.; Verlag Chemie: New York, 1990; p 33.
- Gleiter, R.; Gygax, R. *Topics in Current Chemistry*; Springer-Verlag: Berlin, 1976; p 49.
- Lozac'h, N. *Advances in Heterocyclic Chemistry*; Katritzky, A. R., Boulton, A. J., Eds.; Academic Press: New York, 1971; p 161.
- Arduengo, A. J., III; Burgess, E. M. *J. Am. Chem. Soc.* 1977, 99, 2376.
- Martin, J. C.; Granoth, I. *J. Am. Chem. Soc.* 1979, 101, 4623.
- Granoth, I.; Martin, J. C. *J. Am. Chem. Soc.* 1978, 100, 7434.
- Arduengo, A. J., III; Dixon, D. A. *Electron Rich Bonding at Low Coordination Main Group Element Centers*. In *Heteroatom Chemistry: ICHAC-2*; Block, E., Ed.; VCH: New York, 1990; p 47.
- Arduengo, A. J., III; Dixon, D. A.; Roe, D. C. *J. Am. Chem. Soc.* 1986, 108, 6821.
- Martin, J. C. *Topics in Organic Sulfur Chemistry*; Tisler, J., Ed.; Ljubljana: Yugoslavia, 1978; Chapter 8.
- Martin, J. C.; Perozzi, E. F. *Science*, 1976, 191, 154.
- Culley, S. A.; Arduengo, A. J., III. *J. Am. Chem. Soc.* 1985, 107, 1089.
- Stewart, C. A.; Harlow, R. L.; Arduengo, A. J., III. *J. Am. Chem. Soc.*, 1985, 107, 5543.
- Stewart, S. A.; Arduengo, A. J., III. *J. Am. Chem. Soc.* 1984, 106, 1164.

- (21) Bonningue, C.; Houalla, D.; Sanchez, M.; Wolf, R. *J. Chem. Soc., Perkin Trans. 2* 1981, 19.
- (22) Wolf, R. *Pure Appl. Chem.*, 1980, 52, 1141.
- (23) Houalla, D.; Osman, F. H.; Sanchez, M.; Wolf, R. *Tetrahedron Lett.* 1977, 35, 3041.
- (24) Bonningue, C.; Houalla, D.; Wolf, R. *J. Chem. Soc., Perkin Trans. 2* 1983, 773.
- (25) Arduengo, A. J., III; Stewart, C. A.; Davidson, F.; Dixon, D. A.; Becker, J. Y.; Culley, S. A.; Mizzen, M. B. *J. Am. Chem. Soc.* 1987, 109, 627.
- (26) Murillo, A.; Chiquete, M. L.; Joseph-Nathan, P.; Contreras, R. *Phosphorus, Sulfur, Silicon* 1990, 53, 87.
- (27) Contreras, R. *Phosphorus Sulfur Relat. Elem.* 1994, in press.
- (28) The symbol  $\{\text{ADPO}\}_2$  is used to represent the tricyclic dimer of ADPO (6) in which two molecules dimerize through the P-O bonds of the original five-member ring.
- (29) Levy, G. C.; Lichter, R. L. *Nitrogen-15 Nuclear Magnetic Resonance Spectroscopy*; Wiley: New York, 1979.
- (30) Arduengo, A. J., III; Breker, J.; Davidson, F.; Kline, M. *Heteroat. Chem.* 1993, 4, 213.
- (31) Newton, M. G.; Collier, J. E.; Wolf, R. *J. Am. Chem. Soc.* 1974, 96, 6888.
- (32) This drawing is the result of a local density functional theory (LDF) calculation on 3,7-dimethyl-5-aza-2,8-dioxa-1-phosphabicyclo-[3.3.0]octa-2,4,6-triene. The calculation was done with the program DGauss (TZVP basis set), a density functional program available via the Cray Unichem Project. The outermost contour is at 0.75 eÅ<sup>-3</sup> and the innermost is 10 eÅ<sup>-3</sup> with an interval of 0.3 eÅ<sup>-3</sup> between adjacent contours. We appreciate the help and assistance of Dr. David A. Dixon and Scott C. Walker in making this picture.
- (33) The oxidation state (o.s.) of a central atom described by an N-X-L designator can be calculated as by the relation o.s. = -N + [X] + 2L, where N and L have the usual meanings (see ref 2) and [X] is the number of valence electrons at the isolated atom X. Thus for 10-P-3 ADPO the oxidation state of phosphorus is -10 + 5 + 2(3) or 1. The oxidation state of phosphorus in 8-P-3 ADPO is -8 + 5 + 2(3) or 3. The oxidation state of phosphorus in a 6-P-1 phosphinidene is -6 + 5 + 2(1) or 1.
- (34) This drawing was made with the KANVAS computer graphics program. This program is based on the program SCHAKAL of E. Keller (Kristallographisches Institute der Universität Freiburg, Germany), which was modified by A. J. Arduengo, III (DuPont Science and Engineering Laboratory, Wilmington, DE) to produce the back and shadowed planes. The planes bear a 50-pm grid and the lighting source is at infinity so that shadow size is meaningful.
- (35) Dixon, D. A.; Arduengo, A. J., III; Fukunaga, T. *J. Am. Chem. Soc.* 1986, 108, 2461.
- (36) Dixon, D. A.; Arduengo, A. J., III. *J. Phys. Chem.* 1987, 91, 3195.
- (37) Dixon, D. A.; Arduengo, A. J., III. *J. Chem. Soc., Chem. Commun.* 1987, 1987, 498.
- (38) Arduengo, A. J., III. *Pure Appl. Chem.* 1987, 59, 1053.
- (39) Arduengo, A. J., III; Dixon, D. A.; Roe, D. C.; Kline, M. *J. Am. Chem. Soc.* 1988, 110, 4437.
- (40) Martin, J. C.; Stevenson, W. H., III; Lee, D. Y. *Organosilicon and Biorganosilicon Chemistry*; Sakurai, H., Ed.; Halsted Press: New York, 1985; p 298.
- (41) Akiba, K.-Y.; Chen, X.; Yamamoto, Y. *J. Am. Chem. Soc.* 1992, 114, 7906.
- (42) Gordon, M. S.; Schmidt, M. W. *J. Am. Chem. Soc.* 1993, 115, 7486.
- (43) Karaghiosoff, K.; Schmidpeter, A. *Phosphorus Sulfur* 1988, 36, 217.
- (44) Culley, S. A. Ph.D. Thesis, University of Illinois—Urbana, 1984.
- (45) Reid, D. H.; Webster, R. G. *J. Chem. Soc., Perkins Trans. 1* 1975, 2097.
- (46) Schmidpeter, A.; Weinmaier, J. H. *Angew. Chem., Int. Ed. Engl.* 1975, 14, 489.
- (47) Dieters, J. A.; Gallucci, J. C.; Clark, T. E.; Holmes, R. R. *J. Am. Chem. Soc.* 1977, 99, 5461.
- (48) Holmes, R. R. *Pentacoordinated Phosphorus*, ACS Monograph 175; American Chemical Society: Washington, DC, 1980.
- (49) Arduengo, A. J., III; Dias, H. V. R. Unpublished results, 1992.
- (50) Martin, G.; Martin, N. L.; Gouesnard, J.-P. <sup>15</sup>N-NMR Spectroscopy. In *Nuclear Magnetic Resonance*; Diehl, P., Fluck, E., Kosfeld, R., Eds.; Springer-Verlag: New York, 1981; p 127.
- (51) Hendrickson, J. B.; Spenger, R. E.; Simes, J. J. *Tetrahedron* 1963, 19, 707.
- (52) Reddy, G. S.; Weis, C. D. *J. Org. Chem.* 1963, 28, 1822.
- (53) Forbus, T. R., Jr.; Martin, J. C. *J. Am. Chem. Soc.* 1979, 101, 5057.
- (54) Simmons, H. E.; Fukunaga, T. *J. Am. Chem. Soc.* 1967, 89, 5208.
- (55) Gordon, M. D.; Fukunaga, T.; Simmons, H. E. *J. Am. Chem. Soc.* 1976, 98, 8401.
- (56) Huttner, G.; Müller, H.-D. *Angew. Chem., Int. Ed. Engl.* 1975, 14, 571.
- (57) Bruzik, K.; Stec, W.; Houalla, D.; Wolf, R. *J. Chem. Res. (S)* 1981, 348.
- (58) Koenig, M.; Kläbe, A.; Munoz, A.; Wolf, R. *J. Chem. Soc., Perkins Trans. 2* 1979, 40.
- (59) Arduengo, A. J., III; Dias, R.; Calabrese, J. C., *Phosphorus Sulfur Silicon* 1994, 87, 1.
- (60) Arduengo, A. J., III; Stewart, C. A.; Davidson, F. *J. Am. Chem. Soc.* 1986, 108, 322.
- (61) Bettermann, G.; Arduengo, A. J., III. *J. Am. Chem. Soc.* 1988, 110, 877.
- (62) Arduengo, A. J., III; Lattman, M.; Calabrese, J. C.; Fagan, P. J. *Heteroat. Chem.* 1990, 1, 407.
- (63) Arduengo, A. J., III; Lattman, M.; Dixon, D. A.; Calabrese, J. C. *Heteroat. Chem.* 1991, 2, 395.
- (64) Arduengo, A. J., III; Lattman, M.; Dias, H. V. R.; Calabrese, J. C.; Kline, M. *J. Am. Chem. Soc.* 1991, 113, 1799.
- (65) Shriver, D. F.; Whitmire, K. H. Iron Compounds without Hydrocarbon Ligands. In *Comprehensive Organometallic Chemistry*; Wilkinson, G., Stone, F. G. A., Abel, E. W., Ed.; Pergamon: Oxford, 1982; p 289.
- (66) Reckziegel, A.; Bigorgne, M. *J. Organomet. Chem.* 1965, 3, 341.
- (67) King, R. B. *Inorg. Chem.* 1963, 2, 936.
- (68) Cowley, A. H.; Davis, R. E.; Remadna, K. *Inorg. Chem.* 1981, 20, 2146.
- (69) Riley, P. E.; Davis, R. E. *Inorg. Chem.* 1980, 19, 159.
- (70) Kilbourn, B. T.; Raeburn, U. A.; Thompson, D. T. *J. Chem. Soc. (A)* 1969, 1906.
- (71) Bennett, D. W.; Neustadt, R. J.; Parry, R. W.; Cagle, F. W., Jr. *Acta Crystallogr.* 1978, B34, 3362.
- (72) Vierling, P.; Riess, J. G.; Grand, A. *Inorg. Chem.* 1986, 25, 4144.
- (73) Grumbine, S. D.; Chadha, R. K.; Tilley, T. D. *J. Am. Chem. Soc.* 1992, 114, 1518.
- (74) Lehmkühl, H.; Schwickardi, R.; Kruger, C.; Raabe, G. *Z. Anorg. Allg. Chem.* 1990, 581, 41.
- (75) Straus, D. A.; Tilley, T. D.; Rheingold, A. L.; Geib, S. J. *J. Am. Chem. Soc.* 1987, 109, 5872.
- (76) Straus, D. A.; Cheng, Z.; Quimbita, G. E.; Grumbine, S. D.; Heyn, R. H.; Tilley, T. D.; Rheingold, A. L.; Geib, S. J. *J. Am. Chem. Soc.* 1990, 112, 2673.
- (77) Stewart, C. A.; Arduengo, A. J., III. *Inorg. Chem.* 1986, 25, 3847.
- (78) Muettterties, E. L.; Alegranti, C. W. *J. Am. Chem. Soc.* 1972, 94, 6386.
- (79) Arduengo, A. J., III; Dias, H. V. R.; Calabrese, J. C. *J. Am. Chem. Soc.* 1991, 113, 7071.
- (80) Chang, F. M.; Jansen, M. *Angew. Chem., Int. Ed. Engl.* 1984, 23, 906.
- (81) Roesky, H. W.; Hofmann, H.; Schimkowiak, J.; Jones, P. G.; Meyer-Bäse, K.; Sheldrick, G. M. *Angew. Chem., Int. Ed. Engl.* 1985, 24, 417.
- (82) Arduengo, A. J., III; Dias, H. V. R.; Calabrese, J. C. *Inorg. Chem.* 1991, 30, 4880.